Journal of Medicinal Chemistry

Article

pubs.acs.org/jmc

Design, Synthesis, and Optimization of Novel Epoxide Incorporating Peptidomimetics as Selective Calpain Inhibitors

Isaac T. Schiefer,[†] Subhasish Tapadar,[†] Vladislav Litosh,[†] Marton Siklos,[†] Rob Scism,[†] Gihani T. Wijewickrama,[†] Esala P. Chandrasena,[†] Vaishali Sinha,[†] Ehsan Tavassoli,[†] Michael Brunsteiner,[†] Mauro Fa',[‡] Ottavio Arancio,[‡] Pavel Petukhov,[†] and Gregory R. J. Thatcher*,[†]

[†]Department of Medicinal Chemistry and Pharmacognosy, University of Illinois College of Pharmacy, University of Illinois at Chicago, 833 S. Wood Street, Chicago, Illinois 60612-7231, United States

[‡]Department of Pathology and Cell Biology, The Taub Institute for Research on Alzheimer's Disease and the Aging Brain, Columbia University, 630W 168th Street, New York, New York 10032, United States

Supporting Information

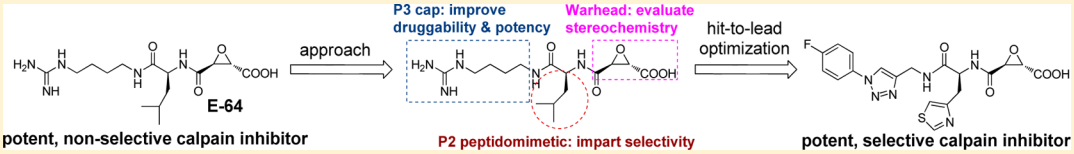

ABSTRACT: Hyperactivation of the calcium-dependent cysteine protease calpain 1 (Cal1) is implicated as a primary or secondary pathological event in a wide range of illnesses and in neurodegenerative states, including Alzheimer's disease (AD). E-64 is an epoxide-containing natural product identified as a potent nonselective, calpain inhibitor, with demonstrated efficacy in animal models of AD. By use of E-64 as a lead, three successive generations of calpain inhibitors were developed using computationally assisted design to increase selectivity for Cal1. First generation analogues were potent inhibitors, effecting covalent modification of recombinant Cal1 catalytic domain ($Cal1_{cat}$), demonstrated using LC−MS/MS. Refinement yielded second generation inhibitors with improved selectivity. Further library expansion and ligand refinement gave three Cal1 inhibitors, one of which was designed as an activity-based protein profiling probe. These were determined to be irreversible and selective inhibitors by kinetics studies comparing full length Cal1 with the general cysteine protease papain.

INTRODUCTION

Calpains are a class of ubiquitously expressed calcium-dependent cysteine proteases that regulate numerous intracellular signaling cascades and are fundamentally involved in regulating protein kinases responsible for cytoskeletal dynamics and remodeling.[1−4] Under physiological conditions, transient and localized Ca^{2+} fluxes from extracellular or intracellular calcium stores result in controlled activation of local calpain populations. While regional calpain proteolytic activity is essential for native Ca^{2+} signaling and cytoskeletal remodeling, pathological conditions may produce excessive levels of Ca^{2+}, resulting in widespread calpain activation and unregulated proteolysis.[5,6] Calpain proteolytic activity contributes to secondary degeneration in situations of acute cellular stress following myocardial ischemia, cerebral ischemia, and traumatic brain injury.[7−10] Enhanced calpain activity in platelets is a contributor to atherothromobosis and diabetes pathology.[11,12] Calpain hyperactivation associated with altered Ca^{2+} homeostasis contributes to pathogenesis of Huntington's disease, Parkinson's disease, cataract formation, glaucoma, multiple sclerosis, and Alzheimer's disease (AD).[5,13−18] In this context, an appropriate selective calpain inhibitor may hold therapeutic potential in selected disease states.

Attempts to develop calpain inhibitors have been cataloged previously.[19,20] The structural nomenclature of cysteine protease substrates and inhibitors is introduced in Figure 1. The majority of reported calpain inhibitors rely upon the ability of an electrophilic reactive group, or "warhead", to either reversibly or irreversibly modify the active site cysteine of calpain. A natural product, E-64, L-*trans*-epoxysuccinylleucylamido(4-guanidino)-butane (Figure 1), was an early identified cysteine protease inhibitor, utilizing an epoxide for active site modification.[21,22] While being nonreactive toward other protease superfamilies (i.e., aspartic, serine, etc.), E-64 serves as a benchmark, high affinity, nonselective, irreversible calpain inhibitor.[23,24] In a transgenic model of AD, E-64 demonstrated excellent in vivo efficacy.[25] Therefore, by use of E-64 as a lead and benchmark, the object of the present study was to maintain potency while increasing Cal selectivity and druggability.

CA clan cysteine proteases (i.e., papain, calpains, and lysosomal cathepsins) have similar P1−P3 substrate binding pockets, which results in a common preference for hydrophobic residues at the S2 subsite (i.e., Leu, Ile, Val, Phe, Tyr).[26,27] It has been suggested that inhibitors containing *S,S* epoxide stereochemistry bind preferentially into the P1−P3 pocket of CA clan proteases.[28,29] Accordingly, E-64 and related *S,S* epoxides containing hydrophobic residues at the P2 position have

Received: February 7, 2013

dx.doi.org/10.1021/jm4006719 | *J. Med. Chem.* XXXX, XXX, XXX−XXX

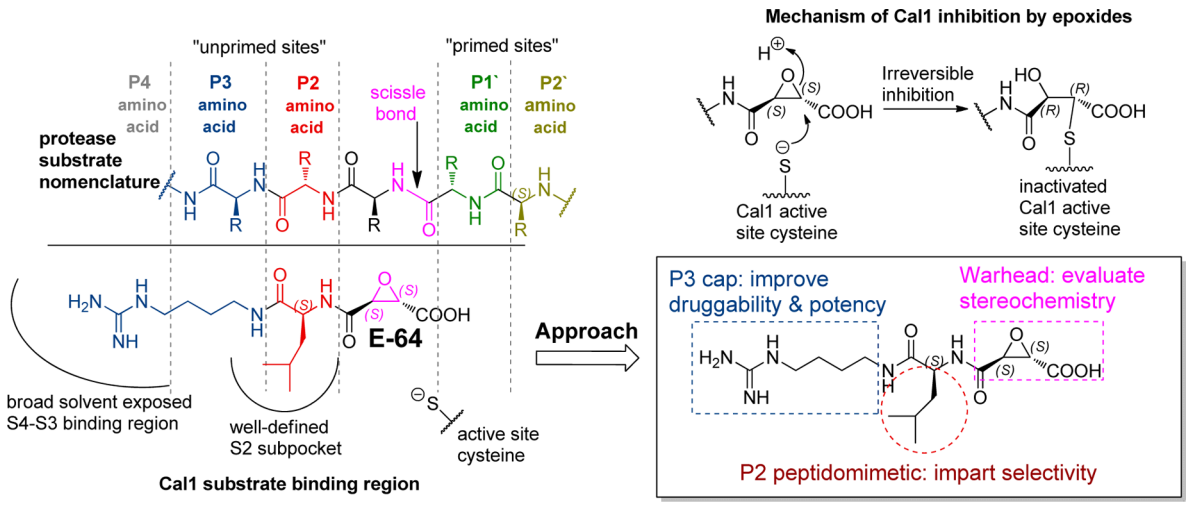

Figure 1. Protease substrates are designated according to their amino acid residues extending from the scissile bond. "Unprimed" and "primed" substrate residues are designated P1, P2, etc. and P1′, P2′, etc., respectively. The design rationale is illustrated using E-64 as a lead.

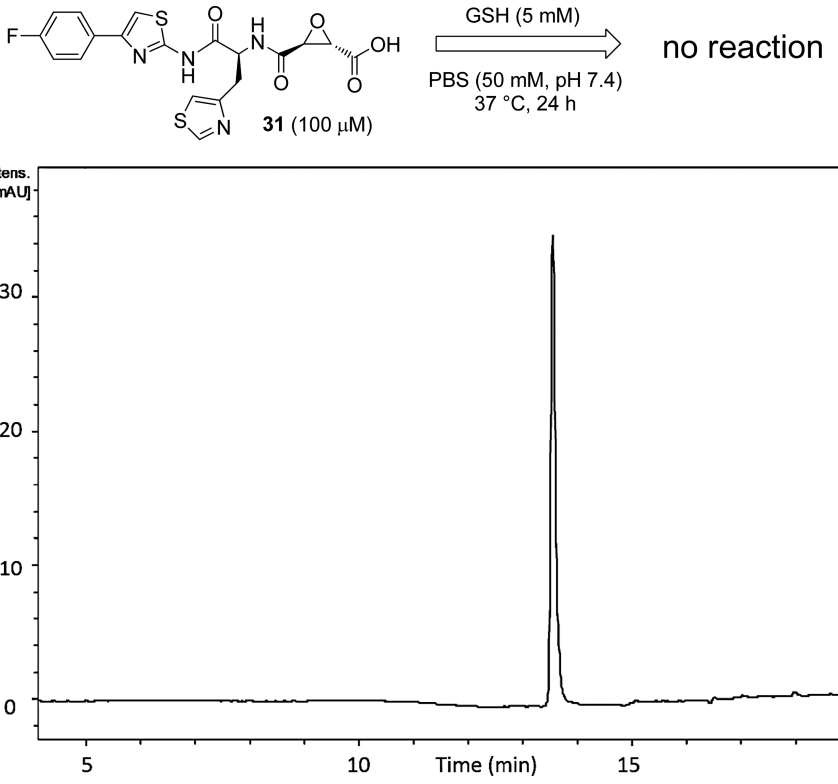

Figure 2. HPLC−UV−vis (λ = 280 nm) chromatogram from incubation of **31** (100 μM) with excess GSH (5 mM) in PBS (50 mM, pH 7.4) at 37 °C for 24 h. Product identity was confirmed using LC−MS/MS and comparison of retention time of authentic sample in the absence of GSH.

shown poor selectivity and good potency for these proteases. Recent efforts examined an array of P4-P3-P2-epoxysuccinate peptides for inhibitory activity against CA clan cysteine proteases, including Cal1, $Cal1_{cat}$ (recombinant calpain 1 catalytic domain), and lysosomal cysteine proteases (cathepsins, Cath).[30] While these peptides do not have optimal druglike properties, their activity profiles give valuable insight into the design and development of novel selective calpain inhibitors using peptidomimetic epoxides. Three successive generations of inhibitors were synthesized using computationally assisted design and Cal1 inhibition data. Modification of the active site cysteine was confirmed using LC−MS/MS and the relative selectivity assessed against papain using an enzyme kinetics analysis. The study presents novel, selective Cal1 inhibitors that because of the presence of the electrophilic epoxide warhead also provide an ideal activity-based protein profiling (ABPP) probe for future mechanistic investigation.

RESULTS AND DISCUSSION

Design and Synthesis. The epoxysuccinate moiety of E-64 is considered essential for potent cysteine protease inhibition. Alternatives to the epoxide warhead, such as alkene and aziridine analogues, possess weak inhibitory activity.[21,31] Despite concerns regarding potential ADMET complications stemming from

dx.doi.org/10.1021/jm4006719 | J. Med. Chem. XXXX, XXX, XXX−XXX

Scheme 1[a]

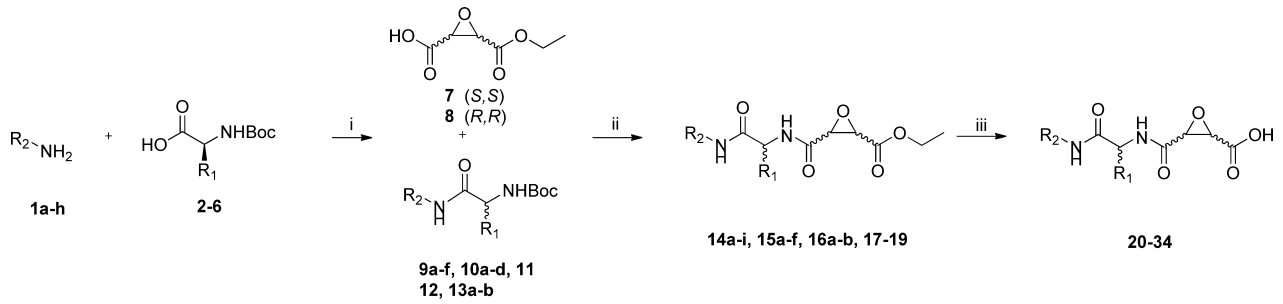

[a]Reagents: (i) EDCI, HOBT, DIPEA, CH_2Cl_2, 0 °C; (ii) EDCI, HOBT, DIPEA, DMF, 0 °C; (iii) LiOH, THF/MeOH/H_2O, 0 °C.

Table 1. Epoxysuccinate Peptidomimetic Structures and Inhibition Data for Full Length Cal1

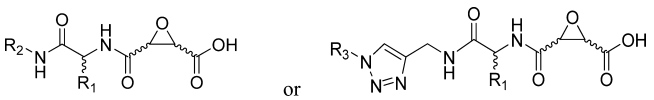

	R_1	R_2 or R_3	epoxide stereochem	Cal1 IC_{50} [a]
E-64	L-leucine	R_2 = guanidinyl-1-pentyl	*S,S*	100 nM
20	L-leucine	R_2 = phenyl	*S,S*	100 nM
21a	L-leucine	R_2 = 2,6-difluorophenyl	*S,S*	100 nM
21b	L-leucine	R_2 = 2,6-difluorophenyl	*R,R*	>1 μM
22a	L-leucine	R_2 = 4-(4-fluorophenyl)thiazol-2-amino	*S,S*	50 nM
22b	L-leucine	R_2 = 4-(4-fluorophenyl)thiazol-2-amino	*R,R*	250 nM
23	L-leucine	R_2 = 4-F-phenyl-SO_2-NH-$(CH_2)_4$-NH	*S,S*	150 nM
24	L-leucine	R_2 = lipoyl-NH-$(CH_2)_4$-NH	*S,S*	100 nM
25	L-leucine	R_2 = D-biotin-NH-$(CH_2)_4$-NH	*S,S*	100 nM
26	L-histidine	R_2 = phenyl	*S,S*	5 μM
27	L-histidine	R_2 = 1,3,5-trimethylanilino	*S,S*	5 μM
28a	L/D-histidine	R_2 = 4-(4-fluorophenyl)thiazol-2-amino	*S,S*	100 nM
28b	L/D-histidine	R_2 = 4-(4-fluorophenyl)thiazol-2-amino	*R,R*	>1 μM[b]
29a	L/D-histidine	R_2 = 6-fluorobenzo[d]thiazol-2-amino	*S,S*	530 nM
29b	L/D-histidine	R_2 = 6-fluorobenzo[d]thiazol-2-amino	*R,R*	>1 μM[b]
30	L-Ala(4-thiazyl)	R_2 = phenyl	*S,S*	2.5 μM
31	L-Ala(4-thiazyl)	R_2 = 4-(4-fluorophenyl)thiazol-2-amino	*S,S*	100 nM
32	L-Ala(4-thiazyl)	R_2 = 4-(4-ethynylphenyl)thiazol-2-amino	*S,S*	100 nM
33	L-His(2-Me)	R_2 = 4-(4-fluorophenyl)thiazol-2-amino	*S,S*	5 μM
34	L-His(4-Me)	R_2 = 4-(4-fluorophenyl)thiazol-2-amino	*S,S*	225 nM
35	L-Ala(4-thiazyl)	R_3 = phenyl	*S,S*	1 μM
36	L-Ala(4-thiazyl)	R_3 = 4-fluorophenyl	*S,S*	100 nM
37	L-Ala(4-thiazyl)	R_3 = 4-(piperidin-1-ylsulfonyl)phenyl	*S,S*	1.5 μM
38	L-Ala(4-thiazyl)	R_3 = benzo[*d*][1,3]dioxol-5-yl	*S,S*	400 nM
39	L-Ala(4-thiazyl)	R_3 = 4-sulfamoylphenyl	*S,S*	>1 μM[b]
40	L-Ala(4-thiazyl)	R_3 = 3,5-bis(trifluoromethyl)phenyl	*S,S*	>1 μM[b]
41	L-Ala(4-thiazyl)	R_3 = 4-bromophenyl	*S,S*	40 nM
42	L-Ala(4-thiazyl)	R_3 = 4-nitrophenyl	*S,S*	300 nM
43	L-Ala(4-thiazyl)	R_3 = 2,6-bis(fluoro)phenyl	*S,S*	>1 μM[b]
44	L-Ala(4-thiazyl)	R_3 = 2,4,6-tris(methyl)phenyl	*S,S*	>1 μM[b]

[a]Inhibition was measured by monitoring fluorescence emission at 480 nm after 20 min incubations with varying concentration of inhibitor in the presence of the FRET substrate: % inhibition normalized to control incubations in the absence of inhibitor. Data represents the mean ± SD of triplicate experiments. [b]Inhibition not quantifiable at 1 μM.

incorporation of the epoxysuccinate moiety, E-64 and derivatives have been approved for clinical studies,[32−34] and there are multiple reports of in vivo efficacy and safety by E-64 and related epoxysuccinate analogues in mice.[35−38] Retention of the epoxysuccinate group also facilitates the design of ABPP probes to identify off-target proteins that may contribute to efficacy or toxicity. Furthermore, we observed that epoxysuccinate containing peptidomimetics show negligible reactivity after 24 h of incubation in the presence of excess GSH at physiological pH and temperature (PBS, 50 mM, pH 7.4, 37 °C; Figure 2). A study describing the low inherent reactivity of the epoxysuccinate moiety with thiols has been reported previously.[39] Given these considerations, the epoxysuccinate moiety was retained and design focused on modifying and evaluating two main portions of the peptidomimetic scaffold: (1) the P3/P4 cap group and (2) the P2 site that is occupied by a L-leucine in E-64.

dx.doi.org/10.1021/jm4006719 | J. Med. Chem. XXXX, XXX, XXX−XXX

Synthesis was directed at generation of a library of peptidomimetic epoxides possessing either natural or non-natural peptidomimetic residues at the P2 position, designated the R_1 substituent, and varying the P3/P4 cap groups, designated as R_2 in Scheme 1. Initially, the R_2-amines were coupled to the commercially available Boc-protected amino acids following typical peptide coupling procedures either using HOBT and EDCI or in the presence of CDI to give the corresponding Boc-protected peptidomimetic scaffolds (**9**−**13**). The epoxysuccinate moiety was synthesized in three steps starting from either L-DET or D-DET, following published procedures to yield the unambiguous epoxysuccinate *R,R* (**7**) and *S,S* (**8**), respectively.[40] Following TFA deprotection, the appropriate peptidomimetic scaffold was coupled to **7** or **8** using EDCI and HOBT in the presence of DIPEA to give the corresponding epoxide esters (**14**−**19**). Ester saponification using LiOH at 0 °C afforded the analogous epoxy acids **20**−**34** (Table 1). In four instances (**28a**,**b** and **29a**,**b**), histidine containing analogues were found to be diastereomeric mixtures (L/D, *S*, *S*) and (L/D, *R*, *R*) resulting from racemization of the peptidyl α-carbon during the initial peptide coupling using CDI.

A limitation in the synthesis of epoxide incorporating inhibitors is the propensity of the epoxide to undergo ring opening. Hence, convergent synthesis is commonly utilized and the epoxide functionality is incorporated after derivatization has taken place, although a divergent synthetic approach is preferred for library development during lead optimization (Scheme 2).

Scheme 2

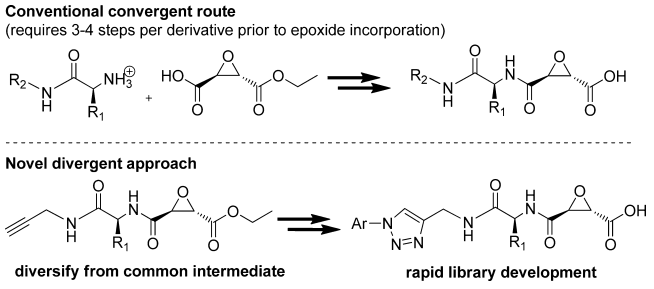

Copper catalyzed Huisgen cycloadditions, also known as "click chemistry", have received much attention because of low cross-reactivity with other functional groups, making it the ideal tool for the generation of a library of epoxide incorporating inhibitors. Computational guidance was employed, vide infra, along with a novel click chemistry route to generate a library of triazole incorporating calpain inhibitors. The key alkynyl intermediate, **19**, was functionalized with arylazides using a Cu[II] catalyzed Huisgen cycloaddition, with the aid of TBTA to give the corresponding triazole aryl incorporating epoxyester peptidomimetics (**35E**−**44E**). Ester saponification yielded the desired epoxyacids (**35**−**44**) in good yield over two steps (85−100%, Scheme 3).

Calpain Inhibition by First Generation Inhibitors: P3/P4 Cap Group Selection. Calpain activity was measured using full-length human Cal1 in the presence of a FRET substrate after 20 min. IC_{50} values were approximated by co-incubation of varying concentrations (10−1000 nM) in the presence of the FRET substrate (DABCYL)TPLK-SPPSPR-(EDANS), and % inhibition was calculated by normalizing to control experiments containing no inhibitor. A peptide inhibitor, Z-LLY-FMK, was used as a positive control.

First generation inhibitors **20**−**25** (Table 1) were designed to mimic E-64 at the P2 position while varying the P3 cap group to increase druggability compared to the ionizable guanidino group of E-64. The majority of first generation inhibitors were found to be approximately equipotent to E-64, and one inhibitor, **22a**, displayed improved potency with an IC_{50} value of 50 nM (±25). These results are consistent with the understanding that hydrophobic amino acid residues at the P2 position deliver high affinity for Cal1. In the instances of **21a**,**b** and **22a**,**b** the importance of the *S,S* epoxide stereochemistry was confirmed.[28,29]

Active Site Modification by Novel Calpain Inhibitors. The recombinant Cal1 catalytic domain ($Cal1_{cat}$) is composed of the proteolytic domain of the full-length enzyme and has been used as a surrogate to study calpain activity.[41−44] $Cal1_{cat}$ provides an advantage because upon Ca^{2+}-induced activation, full length Cal1 engages in autocatalytic, self-proteolysis complicating analysis of activity and inhibition. $Cal1_{cat}$ is devoid of the autocatalytic activity observed for full length Cal1. Recombinant rat $Cal1_{cat}$ was expressed and purified from *E. coli* to examine aspects of inhibition in more detail.

Inhibition kinetics and X-ray crystallography support a mechanism of calpain inhibition by E-64, resulting from covalent modification of the active site Cys.[45] LC−MS/MS supports a similar mechanism for **22a**. The experimental methodology is outlined in Figure 3A. The peptide fragment containing the

Scheme 3[a]

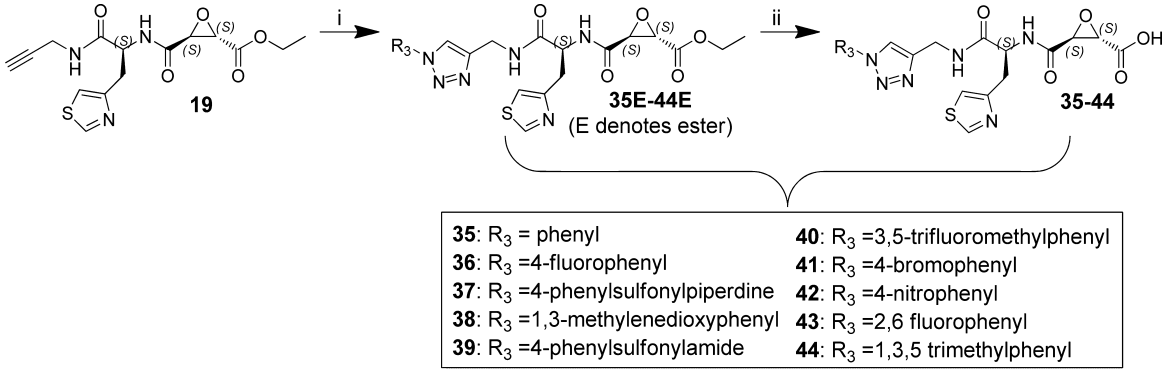

[a]Reagents and conditions: (i) R_3-N_3, $CuSO_4$, NaAsc, TBTA, H_2O/*t*-BuOH/EtOH (2:1:1), rt, 12 h, 90−100%; (ii) LiOH, THF/MeOH/H_2O, 0 °C, 85−100%.

dx.doi.org/10.1021/jm4006719 | J. Med. Chem. XXXX, XXX, XXX−XXX

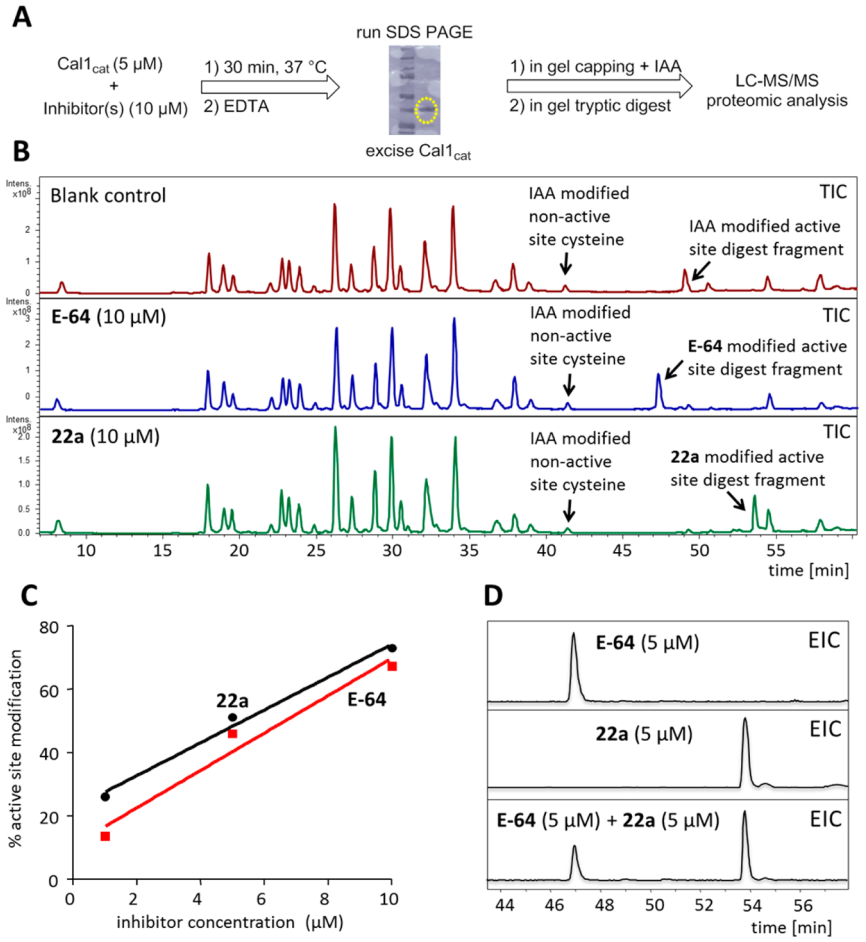

Figure 3. Confirmation of covalent modification of Cal1 active site Cys by epoxysuccinate inhibitors. (A) After in gel digest and capping of free cysteines with iodoacetamide (IAA), peptide fragments were analyzed by LC−MS/MS. (B) Total ion chromatograms (TIC) for the incubation of recombinant $Cal1_{cat}$ (5 μM) in the absence or presence of inhibitors (10 μM). A nonactive site and IAA-capped peptide fragment (t_R = 41.3 min) was used as an internal standard for EIC quantitation. (C) Active site Cys modification of $Cal1_{cat}$ was concentration dependent. (D) Co-incubation of $Cal1_{cat}$ (1 μM) with an inhibitor mixture (5 μM) showed competitive modification of the active site by **22a** and E-64.

active site Cys (TDICQGALGDC*WLLAAIASLTNETILHR) was identified after covalent modification by IAA, **22a**, or E-64. A peptide fragment containing a labeled nonactive site cysteine was used as an internal standard for semiquantitative analysis of the degree of active site modification observed (Figure 3B). It is noteworthy that although $Cal1_{cat}$ was employed in these studies, analysis of full length Cal1 gave an identical active site peptide fragment (TIC of control digest from $Cal1_{cat}$ and full length Cal1 are compared in the Supporting Information).

Incubations of $Cal1_{cat}$ (1 μM) with either E-64 or **22a** showed a concentration dependent modification of the active site cysteine (Figure 3C). Co-incubation of $Cal1_{cat}$ with E-64 and **22a** (both 5 μM) demonstrated relatively greater modification by **22a** (Figure 3D). This outcome, combined with the potency of inhibition by **22a**, supported retention of the 4-*F*-phenylthiazole P3/P4 cap group for subsequent ligand development.

Incorporation of Selectivity in Second Generation Calpain Inhibitors. CA clan cysteine proteases have similar "unprimed" substrate binding pockets, with a common preference for hydrophobic residues at the S2 binding site (i.e., Leu, Ile, Val, Phe).[26,27,29] Previous work on peptides appended with an epoxysuccinate ester warhead has indicated that a P2 histidine might confer Cal1 selectivity, the rationale given being the presence of a stabilizing hydrogen bond occurring within the S2 pocket with a highly conserved water molecule chelated by Glu-349 and Thr-210.[30] A focused series of L-histidine incorporating analogues was synthesized and evaluated (**26**–**29**, **33**, **34**) to probe the S2 pocket.

Facile protonation of the histidine imidazole ring is anticipated to potentially hinder bioavailability; therefore, thiazolyl analogues were also developed (**30**–**32**).[46] Screening of the second generation compounds revealed a general loss of activity on replacement of L-leucine (Table 1), although the P2 analogues, **28a** and **31**, were approximately equipotent to E-64 ($IC_{50} \approx 100$ nM). The crystal structures used to rationalize the selectivity and active site interactions of L-histidine at P2 contained ethyl epoxysuccinate esters, yet in our hands, simple ethyl esters of first and second generation epoxysuccinates did not give measurable inhibition of Cal1 (data not shown).

Target selectivity is the primary goal in mechanism-based drug design; however, for AD pharmacotherapy targeting Cal1, the selection of an off-target enzyme screen needs consideration. Many other cysteine proteases, including proapoptotic caspases, have frequently been proposed as targets for inhibition in AD, dementia, and neurodegenerative disorders.[47,48] Notably, CathB has variously been proposed as a drug target for inhibition in AD therapy.[49−51] The introduction of P2 histidine into epoxysuccinate Cal1 inhibitors by Cuerrier et al. led to selectivity for Cal1 over Cal2, and cathepsins, including CathB. We initially compared E-64, **22a**, and the P2-histidine (**28a**) and thiazolyl

dx.doi.org/10.1021/jm4006719 | J. Med. Chem. XXXX, XXX, XXX−XXX

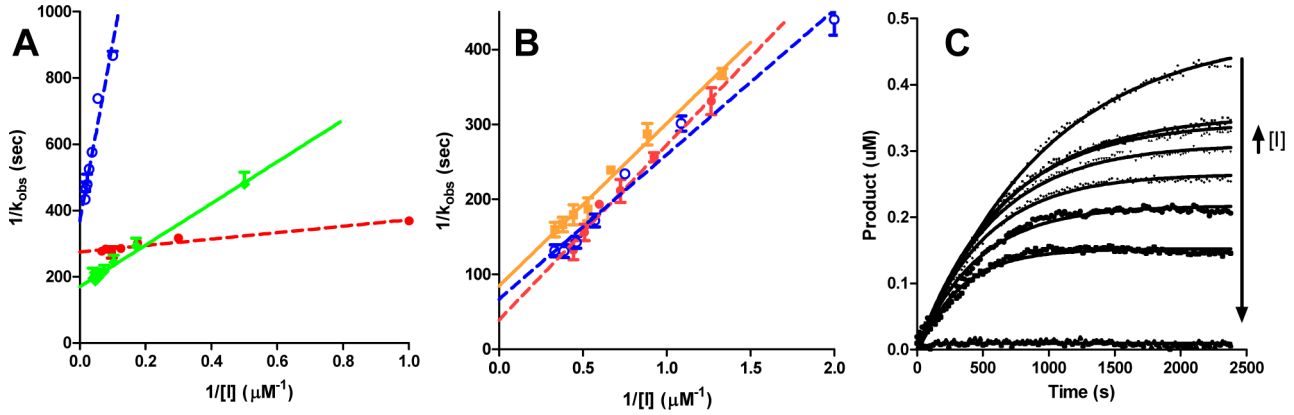

Figure 4. Plots of secondary and primary kinetic data for inhibition of papain (A) and Cal1 (B) used to derive detailed kinetic parameters reported in Table 2: E-64 (diamonds, solid green); **22a** (closed circles, dashed red); **31** (squares, solid orange); **36** (open circles, dashed blue). The observed rate constants (k_{obs}) shown in the double reciprocal plots were measured from nonlinear fitting of "progress curves" for product formation from substrate. Exemplar progress curves are shown for Cal1 inhibition by E-64.

Table 2. Detailed Inhibition Constants for Cal1 and Papain and Relative Inhibitor Selectivity[a]

	calpain 1				papain					
	K_i (μM)	k_i (s^{-1})	k_i/K_i[a] $\times 10^{-4}$ s^{-1} M^{-1}	rel[b]	K_i (μM)	k_i (s^{-1})	k_i/K_i[a] $\times 10^{-4}$ s^{-1} M^{-1}	rel[b]	$10^2 \times$ (k_i/K_i Cal1)/(k_i/K_i papain)	relative selectivity compared to E-64[c]
E-64	3.96	0.12	3.02 ± 0.15	1	5.08	28.6	563 ± 52	1	0.54	1
22a	6.02	0.16	2.74 ± 0.19	0.91	1.62	17.1	1,050 ± 41	1.9	0.26	0.5
31	2.59	0.08	2.96 ± 0.14	0.98	5.31	14.8	279 ± 47	0.50	1.06	2.0
32	3.53	0.14	3.89 ± 0.41	1.3	9.70	21.6	223 ± 2.4	0.40	1.74	3.3
36	2.89	0.10	3.31 ± 0.32	1.1	19.2	12.7	66.2 ± 7.4	0.12	5.0	9.3

[a]Calculated inhibition rate and apparent equilibrium constants versus full length Cal1 and papain. Inhibition constants were calculated as described in the text, varying both enzyme and inhibitor concentrations. Data represent the mean ± SD of triplicate experiments. [b]k_i/K_i calculated relative to E-64. [c]Selectivity calculated using k_i/K_i relative to E-64 set at 1.0.

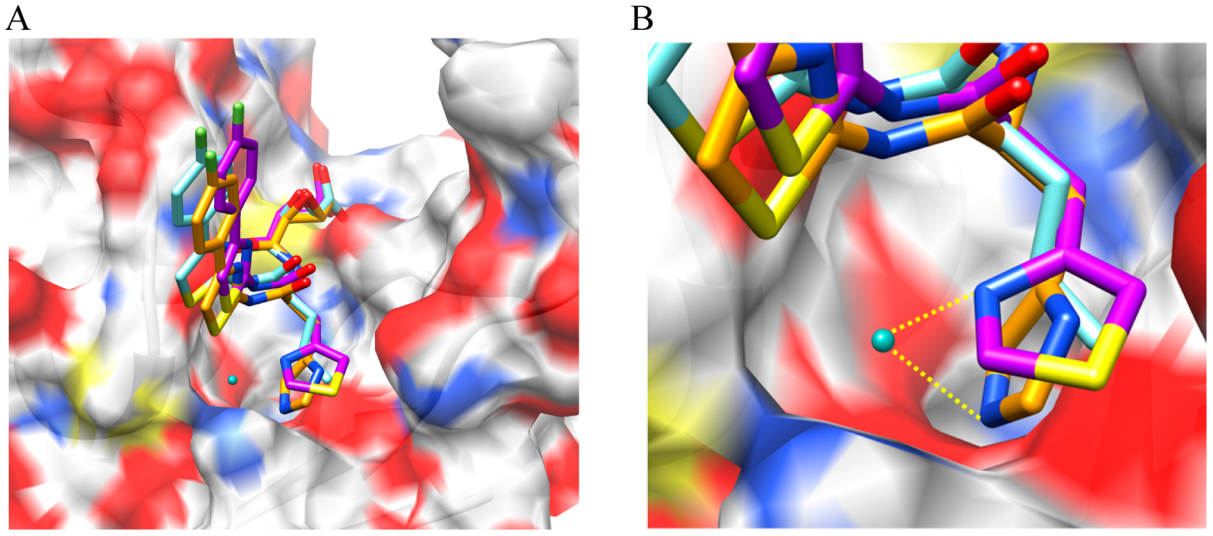

Figure 5. Selected inhibitors (compounds **22a**, **28a**, and **31**) were docked within the WR-18 X-ray structure of $Cal1_{cat}$ [PDB code 2NQG]: (A) structural overlay of putative docking poses; (B) magnified S2 pocket illustrating proposed H-bond formed between the conserved H_2O molecule and the P2 moiety. Docking was carried out using the GOLD docking platform. Docking poses were rendered using UCSF Chimera molecular modeling software.

(**31**) analogues, using an activity directed profiling assay, to confirm the predicted selectivity for Cal1 over CathB (Supporting Information); however, we chose papain for the quantitative counterscreen, as a promiscuous cysteine protease generally representative of the family of typically lysosomal or secreted cysteine proteases, including the human cathepsins (B, C, F, H, K, L1-2, O, S, W, Z).

For papain, the P1 peptide residue is cationic and P2 is hydrophobic and includes Leu; therefore, papain represents a useful counterscreen for Cal1. Several methods have been reported in the literature for detailed kinetic analysis of the

dx.doi.org/10.1021/jm4006719 | J. Med. Chem. XXXX, XXX, XXX−XXX

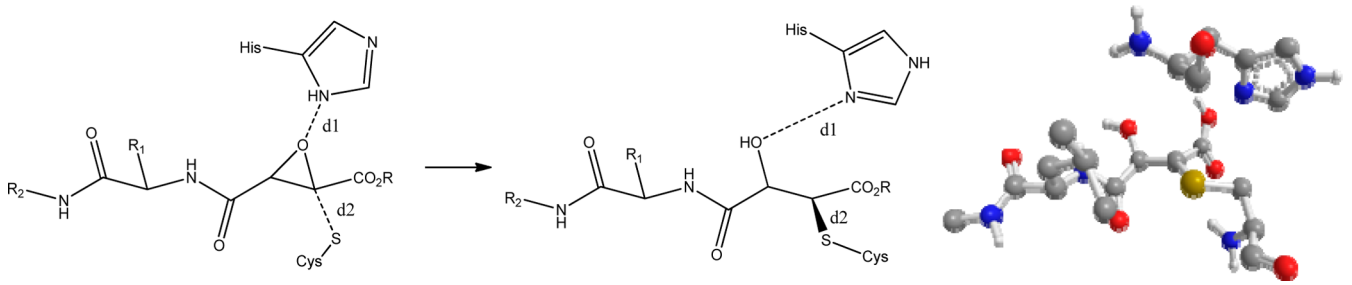

Figure 6. Crystal structures of epoxide inhibitors bound at the active site of Cal1 show a relaxed, ring-opened structure, whereas a transition state for epoxide ring opening requires the Cys nucleophile and His general acid to be aligned for S_N2 substitution. Triazole-based inhibitors were designed based upon docking scores biased toward d2 ≈ 2 Å. For comparison, in the crystal structures, 2NQG has d1 = 4.606 and d2 = 1.810 and 1TLO (shown with E-64, His, and Cys) has d1 = 4.775 and d2 = 1.833.

irreversible inhibition of cysteine proteases, including Cal1. The FRET assay used for initial screening proved to have insufficient signal over noise for detailed kinetic analysis; therefore, conditions were optimized for use of the aminomethylcoumarin substrate SucLLVYAMC. Furthermore, the truncated rat $Cal1_{cat}$ is catalytically inferior to the full length enzyme,[41,42,44] and therefore, full length Cal1 was used for kinetics analysis.

By use of SucLLVYAMC as substrate, kinetics parameters were derived using the method of Davies and co-workers, whereby "progress curves" were initially obtained measuring product formation as a function of time and fitted to $y = P_\infty(1 - e^{(-kx)})$ (Figure 4).[30] Plots of P_∞ versus $1/[I]$ gave excellent linear correlations supporting the validity of the approach (not shown). Kinetics parameters (k_i, K_i, k_i/K_i) were obtained from double reciprocal plots (Table 2). By use of k_i/K_i to assess relative selectivity for inhibition of Cal1 over papain, the data presented in Table 2 show that **22a** is less selective for Cal1 than is the lead compound E-64, whereas **31**, **32**, and **36** all show Cal1 selectivity. Reference to Table 2 and Figure 4 clearly shows that the cause of this selectivity is not enhanced inhibition of Cal1 but attenuated inhibition of papain caused by the P2-thiazole. Thus, introduction of the thiazolyl side chain leads to diminished inhibitory activity against general cysteine proteases as represented by papain while maintaining efficiency for inhibition of Cal1. The P3 cap group of **36** also contributes to the higher selectivity of this derivative by reducing binding affinity to papain but not Cal1.

Structural overlay of docking results for **22a**, **28a**, and **31** predicts a common binding motif, with the P3 cap group extended into the solvent exposed S4−S3 region and the P2 peptidomimetic moiety situated within the S2 pocket (Figure 5). Docking poses are compatible with the potential of **28a** and **31** to interact with the conserved water molecule at the S2 site. It is important to note that incorporation of imidazolyl or thiazolyl groups *did not increase affinity* for the Cal1 binding site relative to the leucine-based inhibitors, as indicated by IC_{50} values.

In Silico Guidance toward P3/P4 Refinement. Computer aided molecular design, based upon crystal structures of cysteine proteases modified by epoxide inhibitors, is expected to be problematic, since nucleophilic attack by the active site Cys thiol leads to ring opening, bond rotations, and relaxation of the resulting ligand−protein adduct. We attempted a variety of docking approaches and programs and found that docking to the X-ray models of the Cal1 that contained a cocrystallized ligand resulted in no correlation between the docking scores and the IC_{50} values. A common assumption for accurate prediction of binding energies of covalently linked ligands is that the binding site and the ligands should undergo minimal conformational changes.[52] This is unlikely to be the case for Cal1 and the epoxide-based ligands. As depicted in Figure 6, reaction at the active site requires close interaction (d2) of the cysteine nucleophile with the electrophilic C2 of the epoxide and probably interaction of the histidine acting as a general acid toward the ring oxygen of the epoxide. In crystal structures of Cal1 adducted with ring-opened inhibitors, gross structural relaxation leads to loss of active site interactions essential for reaction. In addition to these large structural changes expected for unbound and bound epoxide-based ligands, conformational changes to the protein upon ligand binding are expected to be pronounced based on the comparison of X-ray models of Cal1. The conformations of the gating loops[43] in domain I and especially in domain II, which are both part of the binding site and directly interact with the ligands, vary quite dramatically depending on the presence and the structure of the ligand. For example, the gating loop in domain II could be considered "open" in the 2ARY (no ligand), 2G8J, 2NQG, 2NQI, 2R9C, 2R9F (with ligand) and "closed" in 1KXR (no ligand), 1TL9, 1TLO, 1ZCM, 2G8E (with ligand) X-ray structures found in the PDB.

To make use of the structural information, we hypothesized that IC_{50} observed for inhibition of calpain by a covalently bound ligand is proportional to the probability of reaction that in turn is proportional to the number of protein−ligand conformations where such reaction can occur. A conceptually similar approach was successfully used for fast computational prediction of P450 drug metabolism.[53−55] First, we docked a 1,2-substituted ethylene oxide portion general for all the ligands in Table 1 to 2ARY and 1KXR (both are ligand free). The "substrate" was then positioned manually with the assumption that the epoxide should adopt a conformation optimal for nucleophile attack of thiol and its likely interaction with the oxyanion hole formed by the side chain of Gln109. The placement of the non-hydrogen atoms of the oxirane ring was then used to generate rmsd with the corresponding atoms in the docked ligands. To evaluate the probability of reaction using docking, we decided to approximate it as the number of docking poses (NSig) within the rmsd threshold at or below 2 Å. We hypothesized that the higher the number of docking poses complying with this criterion, the better would be the IC_{50}. To test this computational approach and to explore P3/P4 modifications further, a click chemistry route was used to generate a virtual library of analogues of compound **31**, using a divergent synthetic strategy (Scheme 2). Thirty-two synthetically accessible analogues of compound **31** were screened in silico to select 10 for synthesis and assay (Scheme 3). We found that compounds with low NSig values, and therefore predicted to be poor inhibitors (**39**, **40**, **43**, and

dx.doi.org/10.1021/jm4006719 | J. Med. Chem. XXXX, XXX, XXX−XXX

44), yielded relatively poor IC_{50} values, whereas compounds with high NSig, and therefore predicted to be effective inhibitors, displayed higher activity against calpain (**36**, **38**, **41**, and **42**). These promising results require further validation with a larger set of ligands and suggest that this approach originally developed for phase I metabolic enzymes may have broader application.

CONCLUSION

Calpain inhibition has been proposed as a promising therapeutic intervention in many disease states associated with disrupted Ca signaling and hyperactivated Cal1, including neuronal stress leading to neurodegeneration. E-64 and simple analogues have been reported to display in vivo efficacy in murine models of muscular dystrophy and AD; however, the nonselective nature of these compounds is seen as unfavorable for clinical use. Exploiting E-64 as a lead compound, novel peptidomimetic epoxides were designed and generated as Cal1 inhibitors. Active site modification was confirmed by LC−MS/MS. The negligible reactivity toward GSH of epoxysuccinate containing peptidomimetics contrasted with the observed covalent modification of the active site cysteine of Cal1. Potency was maintained via incorporation of the correct epoxide stereochemistry and a 4-F-phenylthiazole P3 cap group (**22a**), allowing selectivity to be achieved by incorporating a P2 thiazolyl group (**31**). Diversity was achieved by developing a divergent synthetic route leading to **36**. Increased selectivity for Cal1 was an objective of this study; however, several cysteine proteases, including caspases and Cath B, have been proposed as targets for AD, dementia, and neurodegenerative disorders[47−51] and would not be appropriate counterscreens predictive of adverse effects. Therefore, papain was used as a counterscreen for selectivity. Retention of the electrophilic epoxide in the present work was deemed as important for the preparation of a Cal1 inhibitor (**32**) that could be used in future studies as an ABPP chemical probe for identification of on-target and off-target proteins to aid in further refinement of both drug targets and drug optimization. Several inhibitors reported herein have shown activity in AD mouse models, and these results in addition to toxicity data will be presented in subsequent manuscripts.

EXPERIMENTAL SECTION

Calpain Inhibition FRET Assay. The Calbiochem InnoZyme activity kit was used for measuring the inhibition effect inhibitors on human erythrocyte calpain 1 activity. A calpain FRET substrate, (DABCYL)-TPLKSPPPSPR-(EDANS), was used to detect the activity of Cal1. 20 μM FRET substrate, 10 nM of native Cal1, and 20 μM TCEP (reducing agent) were added to the reaction mixture containing assay buffer (Tris [10 mM], NaCl [100 mM], pH 7.4). Cal1 was activated by the addition of 10 μM calcium. Cleavage of the scissile bond amide bond, K−S, releases the fluorophore (EDANS) from the internal quenching molecule (DABCYL), resulting in an increase in fluorescence measured at 320 nm excitation and 480 nm emission wavelengths for 20 min. Each inhibitor was added to the reaction mixture at varying concentrations (10 nM, 100 nM, 1 μM, and 10 μM) to detect inhibition of Cal1, and reduction in fluorescence was measured by 96-well plate reader. Approximate IC_{50} values of each compound were generated using linear regression within Graphpad Prism software.

LC−MS/MS Examination of Inhibitor Modified $Cal1_{cat}$ Active Site. Expression from *E. coli* and purification protocols can be found in Supporting Information. Method A refers to the data shown in Figure 3A,B, and method B describes the semiquantitative approach shown in Figure 3C,D. The recombinant $Cal1_{cat}$ (method A, 5 μM; method B, 1 μM) was activated via addition of $CaCl_2$ (10 mM) and incubated with either method: for method A, E-64 or **22a** (10 μM) for 30 min; for method B, E-64 and/or **22a** (1, 5, 10 μM) for 20 min. The competition experiments from Figure 2D were only examined at 5 μM E-64 and **22a**. The reaction was quenched with EDTA (10 μM), and the reaction mixture ran on a SDS−PAGE gel. The $Cal1_{cat}$ containing band was cut from the gel and submitted to in-gel alkylation with IAA (100 mM) for 60 min, followed by trypsin digestion. LC−MS/MS was carried out on an Agilent 6300 ion-trap LC−MS instrument. HPLC separation employed a Phenomenex Jupiter reverse phase HPLC column (5 μm, 150 mm, 2.00 mm); mobile phase ACN (0.1% formic acid)/water (0.1% formic acid). The resulting TIC and EIC were analyzed for anticipated m/z modified peptide fragments. Chromatograms are shown in Figure 3, and m/z peak assignments are included in the Supporting Information.

Calpain and Papain Inhibition Kinetics Studies. Full length porcine calpain (156 nM) or papain (236 pM) was added to a solution of 100 mM NaCl, 50 mM HEPES, pH 7.6, 1 mM TCEP, 30 μM Suc-LLVY-AMC substrate, and inhibitor (0.5−50 μM). Calpain reactions also contained $CaCl_2$ (1 and 100 mM for porcine and rat, respectively). Both substrate and inhibitors were dissolved in acetonitrile/DMSO (1:1) with the exception of E-64, dissolved in water. Organic solvent remained <2% in all reactions and most often <1%. Reactions were carried out in microtiter 96-well plates, with 150 μL per well, 30 °C, and product formation was monitored over time by fluorescence (excitation and emission of 346 and 444 nm, respectively, with 420 nm cutoff filter). Kinetics values of k_{obs} were determined via nonlinear regression using one-phase association analysis, and linear plots of $1/k_{obs}$ vs $1/[I]$ provided kinetics constants k_i and K_i. Representative primary data are supplied in Supporting Information.

Synthesis. General Methods. Unless stated otherwise, all reactions were carried out under an atmosphere of dry argon in oven-dried glassware. Indicated reaction temperatures refer to those of the reaction bath, while room temperature (rt) is noted as 25 °C. Dichloromethane (CH_2Cl_2) was distilled over CaH_2, and THF was distilled over Na(s). All other solvents were of anhydrous quality purchased from Aldrich Chemical Co. and used as received. Pure reaction products were typically dried under high vacuum in the presence of phosphorus pentoxide. Commercially available starting materials and reagents were purchased from Aldrich, TCI, and Fisher Scientific and were used as received unless specified otherwise. Analytical thin layer chromatography (TLC) was performed (column dimensions of 5 cm × 20 cm, 60 Å, 250 μm). Visualization was accomplished using a 254 nm UV lamp. ^1H and ^{13}C NMR spectra were recorded on either a Bruker Avance 400 MHz spectrometer or Bruker DPX 400 MHz spectrophotometer. Chemical shifts are reported in ppm with the solvent resonance as internal standard ($CDCl_3$ at 7.27 and 77.23 ppm, DMSO-d_6 at 2.5 and 39.51 ppm, and MeOD-d_4 at 4.78 and 49.0 for ^1H and ^{13}C, respectively). Data are reported as follows: chemical shift, multiplicity (s = singlet, d = doublet, dd = doublet of doublet, t = triplet, q = quartet, br = broad, m = multiplet, abq = ab quartet), number of protons, and coupling constants. Low-resolution (LR) mass spectra were acquired on an Agilent 6300 ion-trap LC−MS instrument. High resolution mass spectral data were collected in-house using a Shimadzu QTOF 6500. All reported compounds were fully characterized by ^1H NMR and ^{13}C NMR. The structures of all novel final compounds were supported by HRMS. All compounds submitted for biological testing were confirmed to be >95% pure by analytical HPLC. Synthetic procedures, tabulated spectral data, HRMS, and purity analysis for final compounds and novel intermediates are described below. Consult the Supporting Information for extended synthetic procedures and characterization data.

HPLC Analysis of Stability/Reactivity. **31** (100 μM) was incubated with reduced glutathione (5 mM) in PBS (50 mM, pH 7.4, [2% DMSO v/v]) in a temperature controlled HPLC autosampler (37 °C) and reaction progress monitored via 20 μL injections every hour for 24 h. Product identity was confirmed using LC−MS/MS and comparison of retention time of authentic sample in the absence of GSH.

Optimized Procedure for the Coupling of Arylamines to N-Protected Peptidomimetics. A round-bottom flask was charged with the appropriate Boc-protected carboxylic acid (1.0 equiv) dissolved in minimal DMF (~3 mL/mmol) under argon and maintained at 0 °C. EDCI (1.2 equiv) was then added in one portion and the suspension

dx.doi.org/10.1021/jm4006719 | J. Med. Chem. XXXX, XXX, XXX−XXX

stirred until homogeneous (typically <5 min), followed by the addition of HOBt (1.5 equiv). After the mixture was stirred for an additional 15 min, the amine (1.0 equiv) in DMF (~2 mL/mmol) was added dropwise, and the mixture was allowed to warm to room temperature, monitored by TLC. In instances when the amine remained on TLC after 8 h, the mixture was again brought to 0 °C, and additional EDCI (0.5 equiv) was added, followed by stirring for an additional 4 h. The mixture was acidified to pH ≈ 4 with 1 N HCl and extracted with CH_2Cl_2 (3×). Combined organic extracts were washed with 1 N HCl (2×) and brine (1×), dried over Na_2SO_4, concentrated in vacuo, and purified by column chromatography to give the desired peptidomimetic scaffolds.

General Procedure for Coupling of the Epoxide Monoester with the Peptidomimetic Amine. TFA (10 equiv) was added to a suspension of the Boc protected peptidomimetic (1 equiv) in CH_2Cl_2 (20 mL/1 mmol peptidomimetic) at 0 °C and the reaction mixture stirred at the same temperature for 2 h. Excess TFA and CH_2Cl_2 were removed under vacuum and the residual TFA salt was either dried under high vacuum and subjected to the next reaction without further purification or dissolved in MeOH/H_2O and brought to a pH of ~7 using a saturated $NaHCO_3$ solution, followed by extraction with CH_2Cl_2 (3 × 50 mL) and removal of solvent in vacuo to afford the pure free amine, which was used without further purification. The intermediate deprotected amine (1 equiv), the epoxide monoester (1 equiv), and HOBt (1.1 equiv) were dissolved in minimal DMF, and then DIPEA (1 mL, 5.6 mmol) and EDCI (326 mg, 1.7 mmol) were added. After the mixture was stirred at ambient temperature for 12 h, H_2O was added to the reaction mixture and the mixture was diluted with 200 mL of CH_2Cl_2. The organic layer was separated and washed with 1 N HCl (20 mL), saturated $NaHCO_3$ solution (10 mL), water (30 mL), brine (10 mL), dried over anhydrous Na_2SO_4, and concentrated in vacuo. Chromatographic purification of the crude mixture gave the title compounds.

Optimized Procedure for Coupling of the Epoxide Monoester with the Peptidomimetic Amine Boc Deprotection: TFA (10 equiv) was added to a suspension of the appropriate Boc-protected peptidomimetic (1 equiv) in freshly distilled CH_2Cl_2 (10 mL/1 mmol peptidomimetic) at 0 °C and the reaction mixture stirred at the same temperature for 6 h. If needed, additional TFA (5 equiv) was added at 0 °C every 30 min until no starting material remained on TLC. The mixture was then concentrated in vacuo, and the residual TFA salt was dissolved in MeOH/H_2O and brought to pH ≈ 7 using a saturated $NaHCO_3$ solution, followed by extraction with CH_2Cl_2 (3 × 50 mL), and removal of solvent in vacuo to afford the pure free amine, which was dried under high vacuum and used in the next reaction without further purification.

Coupling. A round-bottom flask was charged with the appropriate epoxide monoacid (1.0 equiv) dissolved in minimal DMF (~2 mL/mmol) with DIPEA (1.1 equiv) under argon and maintained at 0 °C. EDCI (1.0 equiv) was then added in one portion and the suspension stirred until homogeneous (typically <5 min), followed by the addition of HOBt (1.2 equiv). After the mixture was stirred for an additional 15 min, the free amine (1.0 equiv) in DMF (~3 mL/mmol) was added dropwise, and the mixture was allowed to warm to room temperature, monitored by TLC. After 12 h, the reaction was quenched acidified to pH ≈ 4 with 1 N HCl, extracted with CH_2Cl_2 (3×). Combined organic extracts were washed with 1 N HCl (2×), and brine (1×), dried over Na_2SO_4, concentrated in vacuo, and purified by column chromatography to give the desired peptidomimetic scaffolds.

General Procedure for Peptidomimetic Epoxide Ester Saponification. The peptidomimetic epoxide ester (1 equiv) was dissolved in THF/MeOH/H_2O (3:1:1) and cooled to 0 °C, and LiOH (1 equiv) was added. The mixture was allowed to warm to room temperature. Additional LiOH (0.2 equiv) was added at 0 °C every 3 h as needed until no starting material remained on TLC. The resulting solution was acidified with cold 1 N HCl and poured into CH_2Cl_2. In some cases the acid precipitated out and was filtered through a sintered funnel and washed consecutively with CH_2Cl_2 and H_2O and isolated. In instances when the compound stayed in solution, the aqueous phase was extracted with CH_2Cl_2 (3 × 50 mL), and the combined organic extracts were dried over Na_2SO_4 and concentrated to give the desired product. Typically, the purity of the desired product reflects the purity of the ester starting material. It was found that having sufficiently pure ester starting material is essential to afford a pure acid upon hydrolysis.

(2*S*,3*S*)-3-((*S*)-4-Methyl-1-oxo-1-(phenylamino)pentan-2-ylcarbamoyl)oxirane-2-carboxylic Acid (20). The general procedure was followed using the corresponding peptidomimetic epoxide ethyl ester **14a** (70 mg, 0.2 mmol) and LiOH (4.8 mg, 0.2 mmol) and after extraction afforded the desired product as a white solid (54 mg, 83.9%). ^{1}H NMR (MeOD-d_4, 400 MHz): δ 7.57−7.55 (d, 2H); 7.33−7.29 (t, 2H); 7.13−7.09 (t, 1H); 4.64−4.61 (m, 1H); 3.71 (s, 1H); 3.57 (s, 1H); 1.76−1.65 (m, 3H); 1.02−0.98 (t, 6H). ^{13}C NMR (MeOD-d_4, 100 MHz): δ 171.22, 169.07, 167.14, 137.98, 128.41, 124.12, 120.14, 52.90, 52.58, 51.69, 40.70, 29.49, 24.64, 22.04, 20.59. ESI-HRMS (m/z) [M − H$^+$] calcd for $C_{16}H_{20}N_2O_5$: 319.3404. Observed: 319.1332. HPLC method 1: t_R = 21.0 min, purity = 96.1%.

(2*S*,3*S*)-3-((*S*)-1-(2,6-Difluorophenylamino)-4-methyl-1-oxopentan-2-ylcarbamoyl)oxirane-2-carboxylic Acid (21a). The general procedure was followed using the corresponding peptidomimetic epoxide ethyl ester **14b** (28 mg, 0.07 mmol) and LiOH (1.7 mg, 0.07 mmol) and after extraction afforded the desired product as a white solid (20 mg, 77.0%). ^{1}H NMR (MeOD-d_4, 400 MHz,): δ 7.91 (s, 1H); 7.36−7.31 (m, 1H); 7.07−7.02 (t, 2H); 4.72 (m, 1H); 3.65 (s, 1H); 3.52 (s, 1H); 1.74−1.68 (m, 3H); 1.01−0.99 (d, 6H). ^{13}C NMR (DMSO-d_6, 100 MHz): δ 171.26, 169.20, 165.81, 159.49 (d, J = 5.2 Hz); 157.00 (d, J = 5.2 Hz); 128.98 (t, J = 19.7 Hz); 115.34 (t, J = 34.0 Hz); 113.10 (d, J = 5.2 Hz); 107.43, 106.22, 52.96, 51.51, 51.32, 41.30, 24.71, 23.81. ESI-HRMS (m/z) [M − H]$^+$ calcd for $C_{16}H_{20}N_2O_5$: 355.3216. Observed: 355.3101. HPLC method 1: t_R = 19.7 min, purity = 95.0%.

(2*R*,3*R*)-3-((*S*)-1-(2,6-Difluorophenylamino)-4-methyl-1-oxopentan-2-ylcarbamoyl)oxirane-2-carboxylic Acid (21b). The general procedure was followed using the corresponding peptidomimetic epoxide ethyl ester **14c** (85 mg, 0.22 mmol) and LiOH (5.2 mg, 0.22 mmol) and after extraction afforded the desired product as a white solid (59 mg, 74.8%). ^{1}H NMR (DMSO-d_6, 400 MHz,): δ 9.88 (s, 1H); 8.81−8.79 (d, 1H, J = 8.21 Hz); 7.38−7.33 (m, 1H); 7.17−7.13 (t, 2H); 4.61−4.56 (q, 1H); 3.70−3.69 (d, 1H, J = 1.79 Hz); 3.52−3.51 (d, 1H, J = 1.79 Hz); 1.66−1.58 (m, 3H); 0.93−0.88 (dd, 6H). ^{13}C NMR (DMSO-d_6, 100 MHz): δ 171.35, 169.20, 165.79, 159.48 (d, J = 5.16 Hz); 157.01 (d, J = 5.21 Hz); 128.58 (t, 19.7 Hz); 114.63 (t, J = 34.0 Hz); 112.39 (d, J = 22.6 Hz); 53.05, 51.71, 51.62, 41.32, 24.71, 21.96. ESI-HRMS (m/z) [M − H$^+$] calcd for $C_{16}H_{20}N_2O_5$: 355.3216. Observed: 355.3201. HPLC method 1: t_R = 18.9 min, purity = 96.5%.

(2*S*,3*S*)-3-((*S*)-1-(4-(4-Fluorophenyl)thiazol-2-ylamino)-4-methyl-1-oxopentan-2-ylcarbamoyl)oxirane-2-carboxylic Acid (22a). The general procedure was followed using the corresponding peptidomimetic epoxide ethyl ester **14d** (203 mg, 0.45 mmol) and LiOH (10.8 mg, 0.45 mmol) and after extraction afforded the desired product as a white solid (150 mg, 78.8%). ^{1}H NMR (DMSO-d_6, 400 MHz): δ 12.51 (bs, 1H); 8.64−8.61 (d, 1H, J = 12.0 Hz); 7.95−7.92 (t, 2H); 7.62 (s, 1H); 7.28−7.24 (t, 2H); 4.63−4.58 (m, 1H); 3.51−3.50 (d, 1H, J = 1.60 Hz); 3.34−3.33 (d, 1H, J = 1.60 Hz); 165−1.54 (m, 3H); 0.91−0.88 (t, 6H). ^{13}C NMR (MeOD-d_4, 100 MHz): 172.44, 165.32, 162.87, 159.37, 150.45, 132.60, 132.57, 129.14, 129.06, 116.56, 116.34, 108.69, 54.41, 53.55, 53.19, 41.79, 26.21, 23.54, 22.02. ESI-HRMS (m/z) [M + H$^+$] calcd for $C_{19}H_{20}FN_3O_5S$: 422.1180. Observed: 422.1188. HPLC method 1: t_R = 24.6 min, purity = 95.7%.

(2*R*,3*R*)-3-((*S*)-1-(4-(4-Fluorophenyl)thiazol-2-ylamino)-4-methyl-1-oxopentan-2-ylcarbamoyl)oxirane-2-carboxylic Acid (22b). The general procedure was followed using the corresponding peptidomimetic epoxide ethyl ester **14e** (76.4 mg, 0.16 mmol) and LiOH (8 mg, 0.34 mmol) and after extraction afforded the desired product as a white solid (51 mg, 71.5%). ^{1}H NMR (DMSO-d_6, 400 MHz): δ 12.52 (s, 1H); 8.78−8.76 (d, 1H, J = 8.0 Hz); 7.94−7.92 (t, 2H); 7.63 (s, 1H); 7.29−7.24 (t, 2H); 4.58−4.57 (m, 1H); 3.62−3.61 (d, 1H, J = 1.80 Hz); 3.41−3.40 (d, 1H, J = 1.80 Hz); 1.64−1.51 (m, 3H); 0.91−0.88 (dd, 6H). ^{13}C NMR (DMSO-d_6, 100 MHz): δ 171.02, 166.26, 162.88, 160.46, 157.72, 147.81, 130.80, 130.77, 127.62, 127.54, 115.59 (d, J = 21.6 Hz); 107.97, 52.36, 52.08, 51.37, 28.89, 24.25, 22.82, 21.19. ESI-HRMS (m/z) [M + H$^+$] calcd for $C_{19}H_{20}FN_3O_5S$: 422.1180. Observed: 422.1186. HPLC method 1: t_R = 23.8 min, purity = 95.1%.

dx.doi.org/10.1021/jm4006719 | J. Med. Chem. XXXX, XXX, XXX−XXX

(2*S*,3*S*)-3-((*S*)-1-(4-(4-Fluorophenylsulfonamido)-butylamino)-4-methyl-1-oxopentan-2-ylcarbamoyl)oxirane-2-carboxylic Acid (23). The general procedure was followed using the corresponding peptidomimetic epoxide ethyl ester **14f** (213 mg, 0.42 mmol) and LiOH (21 mg, 0.85 mmol) and after extraction afforded the desired product as a white solid (110 mg, 54.7%). ^{1}H NMR (DMSO-d_6, 400 MHz): δ 8.15 (s, 1H); 7.89−7.85 (m, 2H); 7.38 (s, 1H); 7.21−7.17 (t, 2H); 6.14 (s, 1H); 3.68−3.60 (d, 2H); 3.38−3.37 (d, 1H, J = 1.60 Hz); 3.10−3.09 (d, 1H, J = 1.60 Hz); 2.97 (s, 1H); 2.85 (s, 1H); 1.65−1.56 (m, 7H); 0.91−0.88 (m, 6H). ^{13}C NMR (DMSO-d_6, 100 MHz): δ 173.41, 170.47, 166.90, 166.52, 163.99, 135.75, 135.72, 130.03, 129.93, 116.71, 116.48, 53.83, 52.32, 43.08, 41.34, 39.65, 26.76, 26.22, 24.95, 22.94, 22.06. ESI-HRMS (m/z) [M + H$^+$] calcd for $C_{20}H_{28}FN_3O_7S$: 474.1705. Observed: 474.1707. HPLC method 1: t_R = 20.9 min, purity = 99.0%.

(2*S*,3*S*)-3-((2*S*)-1-(4-(5-(1,2-Dithiolan-3-yl)pentanamido)-butylamino)-4-methyl-1-oxopentan-2-ylcarbamoyl)oxirane-2-carboxylic Acid (24). **14g** (53 mg, 0.1 mmol) was dissolved in 2 mL of 3:1:1 mixture of THF, methanol, and water and cooled to 0 °C, and LiOH (5 mg, 0.2 mmol) was added. After the mixture was stirred at the same temperature for 15 min the resulting solution was acidified with 1 N HCl and extracted with CH_2Cl_2. The organic layer was washed with water, brine, dried over anhydrous Na_2SO_4, and concentrated in vacuo. Column purification of the crude mixture (SiO_2, 15% MeOH/$CHCl_3$) gave the title compound as a white solid. ^{1}H NMR ($CDCl_3$, 400 MHz): δ 8.01−7.99 (d, 1H, J = 10.8 Hz); 7.26 (s, 1H); 6.25 (bs, 1H); 4.57−4.53 (q, 1H); 3.69 (s, 1H); 3.59 (s, 1H); 3.21−3.31 (m, 5H); 2.45−2.42 (m, 1H); 2.24−2.20 (t, 2H); 1.94−1.92 (m, 1H); 1.66−1.51 (m, 12H); 1.25−1.21 (m, 2H); 0.94−0.91 (m, 6H). ^{13}C NMR ($CDCl_3$, 100 MHz): δ 174.12, 172.13, 168.92, 166.64, 56.52, 53.57, 52.57, 51.62, 41.19, 40.31, 39.09, 38.93, 38.50, 36.24, 34.63, 28.93, 26.56, 26.42, 25.55, 24.85, 22.80, 21.87. ESI-HRMS (m/z) [M + H$^+$] calcd for $C_{22}H_{37}N_3O_6S_2$: 504.2197. Observed: 504.2192. HPLC method 1: t_R = 21.7 min, purity = 95.4%.

(2*S*,3*S*)-3-((*S*)-4-Methyl-1-oxo-1-(4-(5-((3a*S*,4*S*,6a*R*)-2-oxo-hexahydro-1*H*-thieno[3,4-*d*]imidazol-4-yl)pentanamido)-butylamino)pentan-2-ylcarbamoyl)oxirane-2-carboxylic Acid (25). The general saponification procedure was followed using the corresponding peptidomimetic epoxide ethyl ester **14h** (155 mg, 0.3 mmol), LiOH (14 mg, 0.58 mmol), and THF/MeOH/H_2O (1.5 mL/0.5 mL/0.5 mL), yielding **25** as a white solid (40 mg, 27.1%). ^{1}H NMR (DMSO-d_6, 400 MHz): 8.56 (d, 1H); 8.06 (t, 1H); 7.76 (t, 1H); 6.41 (s, 1H), 6.35 (s, 1H); 4.57 (m, 2H); 4.31 (m, 1 H); 3.66 (d, 1H); 3.31 (d, 1H); 3.08 (m, 1H); 3.01 (m, 3H); 2.80 (dd, 1H); 2.56 (d, 1H); 2.04 (t, 2H); 1.53 (m, 6H); 1.43 (m, 3H); 1.36 (m, 2H); 0.89 (d, 3H); 0.84 (d, 3H). ^{13}C NMR (DMSO-d_6, 100 MHz): δ 171.80, 171.06, 168.78, 164.85, 162.68, 61.00, 59.16, 55.36, 52.65, 51.19, 41.14, 35.17, 28.17, 27.98, 26.59, 26.45, 25.28, 24.24, 22.87, 21.61. ESI-HRMS (m/z) no ionization, mass not seen. HPLC method 1: t_R = 14.8 min, purity = 95.6%.

(2*S*,3*S*)-3-((*S*)-3-(1*H*-Imidazol-4-yl)-1-oxo-1-(phenylamino)-propan-2-ylcarbamoyl)oxirane-2-carboxylic Acid (26). The general saponification procedure was followed using the corresponding peptidomimetic epoxide ethyl ester **15a** (155 mg, 0.3 mmol), LiOH (14 mg, 0.58 mmol), and THF/MeOH/H_2O (1.5 mL/0.5 mL/0.5 mL), yielding **26** as a white solid (40 mg, 27.1%). ^{1}H NMR (MeOD-d_4, 400 MHz): δ 8.66 (s, 1H); 7.57−7.55 (d, 2H, J = 7.86 Hz); 7.29−7.27 (t, 3H); 7.10−7.07 (t, 1H); 4.97−4.94 (q, 1H); 3.64−3.63 (d, 1H, J = 1.66 Hz); 3.529−3.525 (d, 1H, J =1.66 Hz); 3.36−3.15 (m, 2H). ^{13}C NMR (MeOD-d_4, 100 MHz): δ 169.79, 167.26, 166.95, 137.90, 134.99, 128.37, 124.10, 120.11, 54.13, 52.94, 51.67. ESI-HRMS (m/z) [M + H$^+$] calcd for $C_{16}H_{16}N_4O_5$: 345.1194. Observed: 345.1185. HPLC method 1: t_R = 18.2 min, purity = 95.2%.

(2*S*,3*S*)-3-((*S*)-3-(1*H*-Imidazol-5-yl)-1-(mesitylamino)-1-oxo-propan-2-ylcarbamoyl)oxirane-2-carboxylic Acid (27). The general saponification procedure was followed using the corresponding peptidomimetic epoxide ethyl ester **15b** (51.6 mg, 0.1 mmol), LiOH (5 mg, 0.2 mmol), and THF/MeOH/H_2O (1.5 mL/0.5 mL/0.5 mL), yielding **27** as a white solid (26.2 mg, 54.2%). ^{1}H NMR (MeOD-d_4, 400 MHz): δ 7.62 (s. 1H); 6.93 (s, 1H); 6.87 (s, 2H); 4.84−4.82 (m, 1H); 3.53−3.49 (d, 1H); 3.38−3.35 (d, 1H); 3.25−3.22 (m, 2H); 2.25 (s, 3H); 2.07 (s, 6H). ^{13}C NMR (MeOD-d_4, 100 MHz): δ 174.40, 172.62, 170.80, 168.89, 136.54, 135.74, 135.11, 133.43, 131.25, 128.18, 117.26, 54.20, 53.82, 53.69, 52.80, 29.34, 19.55, 16.86. ESI-HRMS (m/z) [M − H$^+$] calcd for $C_{19}H_{22}N_4O_5$: 385.1517. Observed: 385.1516. HPLC method 2: t_R = 16.4 min, purity = 95.4%

(2*S*,3*S*)-3-(1-(4-(4-Fluorophenyl)thiazol-2-ylamino)-3-(1*H*-imidazol-4-yl)-1-oxopropan-2-ylcarbamoyl)oxirane-2-carboxylic Acid (28a). The general saponification procedure was followed using the corresponding peptidomimetic epoxide ethyl ester **15c** (184 mg, 0.39 mmol), LiOH (14 mg, 0.58 mmol), and THF/MeOH/H_2O (1.5 mL/0.5 mL/0.5 mL), yielding **28a** as a white solid (40 mg, 27.1%). ^{1}H NMR (DMSO-d_6, 400 MHz): δ 12.50 (bs, 1H); 8.84−8.73 (dd, 1H, J = 7.3 Hz, 7.3 Hz); 7.95−7.91 (q, 2H); 7.73 (s, 1H); 7.63 (s, 1H); 7.29−7.24 (t, 2H); 6.90 (s, 1H); 4.81−4.74 (m, 1H); 3.65−3.64 (dd, 2H, J = 1.68 Hz, 1.68 Hz); 3.46−3.42 (dd, 2H, J = 1.65 Hz, 1.65 Hz); 3.09−3.01 (m, 2H). ^{13}C NMR (DMSO-d_6, 100 MHz): δ 169.81, 165.89, 163.95, 157.92, 147.96, 134.99, 132.93, 132.91, 127.89, 127.72, 115.77, 115.56, 108.17, 99.59, 52.69, 51.85, 51.77. ESI-HRMS (m/z) [M + H$^+$] calcd for $C_{19}H_{16}FN_5O_5S$: 446.0929. Observed: 446.0922. HPLC method 2: t_R = 16.2 min (*S*-isomer) and t_R = 12.8 min (*R*-isomer), purity = 98.2%. For characterization purposes, isomeric identity was determined by resynthesis with the use of HOBT in the initial peptide coupling. This led to isolation of the enantiomerically pure *S*-isomer, which elutes at t_R = 16.2 min, corresponding to the *S*-isomer in the enantiomeric mixture. Only the racemic mixture was tested for potency and selectivity.

(2*R*,3*R*)-3-((*S*)-1-(4-(4-Fluorophenyl)thiazol-2-ylamino)-3-(1*H*-imidazol-4-yl)-1-oxopropan-2-ylcarbamoyl)oxirane-2-carboxylic Acid (28b). The general saponification procedure was followed using the corresponding peptidomimetic epoxide ethyl ester **15d** (200 mg, 0.42 mmol), LiOH (12 mg, 0.50 mmol), and THF/MeOH/H_2O (2.5 mL/1.5 mL/1.5 mL), yielding **28b** as a white solid (85 mg, 45.2%). ^{1}H NMR (DMSO-d_6, 400 MHz,): δ 12.52 (bs, 1H); 8.85−8.75 (dd, 2H, J = 6.9 Hz; J = 43.1 Hz); 7.94−7.91 (t, 2H); 7.80 (s, 1H); 7.62 (s, 1H); 7.28−7.24 (t, 2H); 6.93 (s, 1H); 4.80−4.76 (q, 1H); 3.65−3.64 (d, 1H, J = 4.40 Hz); 3.46−3.42 (d, 1H, J = 14.0 Hz); 3.09−2.96 (m, 2H). ^{13}C NMR (DMSO-d_6, 100 MHz): δ 169.5, 168.8, 165.9, 162.9, 160.5, 157.6, 147.8, 134.6, 132.1, 130.7, 127.6, 116.4, 115.5 (d, J = 21.4 Hz), 108.0, 52.9, 52.7, 52.6, 51.9, 28.6. ESI-HRMS (m/z) [M + H$^+$] calcd for $C_{19}H_{16}FN_5O_5S$: 446.0928. Observed: 446.0939; HPLC method 2: t_R = 15.8 min, purity = 97.2%.

(2*S*,3*S*)-3-((*S*)-1-(6-Fluorobenzo[*d*]thiazol-2-ylamino)-3-(1*H*-imidazol-4-yl)-1-oxopropan-2-ylcarbamoyl)oxirane-2-carboxylic Acid (29a). The general saponification procedure was followed using the corresponding peptidomimetic epoxide ethyl ester **15e** (153 mg, 0.32 mmol), LiOH (7.7 mg, 0.32 mmol), and THF/MeOH/H_2O (3.5 mL/1.5 mL/1.5 mL), yielding **29a** as a white solid (103 mg, 71.5%). ^{1}H NMR (DMSO-d_6, 400 MHz): δ 14.55 (bs, 1H); 14.36 (bs, 1H); 9.18−9.02 (m, 2H); 7.93−7.91 (m, 1H); 7.79−7.75 (m, 1H); 7.44 (s, 1H); 7.31−7.29 (t, 1H); 4.96−4.91 (q, 1H); 3.72−3.71 (d, 1H, J = 1.62 Hz); 3.51−3.50 (d, 1H, J = 1.62 Hz); 3.29−3.16 (m, 2H). %). ^{13}C NMR (DMSO-d_6, 100 MHz): δ 169.50, 168.51, 165.84, 165.84, 159.82, 157.53, 157.44, 145.02, 133.67, 132.68, 132.57, 128.56, 121.63, 117.01, 114.40, 114.16, 108.27, 108.00, 52.67, 52.19, 51.34, 26.20. ESI-HRMS (m/z) [M + H$^+$] calcd for $C_{17}H_{14}FN_5O_5S$: 420.0773. Observed: 420.0777.

(2*R*,3*R*)-3-((*S*)-1-(6-Fluorobenzo[d]thiazol-2-ylamino)-3-(1*H*-imidazol-4-yl)-1-oxopropan-2-ylcarbamoyl)oxirane-2-carboxylic Acid (29b). The general saponification procedure was followed using the corresponding peptidomimetic epoxide ethyl ester **15f** (125 mg, 0.26 mmol), LiOH (6.2 mg, 0.26 mmol), and THF/MeOH/H_2O (1.5 mL/1.0 mL/0.5 mL), yielding **29b** as a white solid (46 mg, 39.1%). ^{1}H NMR (400 MHz, MeOD-d_4): δ 11.88 (bs, 1H), 8.89−8.83 (dd, 1H, J = 7.4 Hz, J = 7.4 Hz); 7.91−7.89 (d, 1H, J = 2.5 Hz); 7.78- 7.72 (q, 1H); 7.56 (s, 1H); 7.30 (td, 1H, J = 2.6 Hz); 6.85 (s, 1H); 4.81−4.76 (m, 1H); 3.76−3.74 (dd, 1H, J = 1.68 Hz); 3.45−3.43 (dd, 1H, J = 1.65 Hz); 3.11−3.00 (m, 2H). ^{13}C NMR (DMSO-d_6, 100 MHz): δ 171.13, 167.48, 165.83, 160.32, 158.21, 145.64, 135.40, 133.23, 122.17, 114.83, 108.74, 53.86, 53.40, 51.86. ESI-HRMS (m/z) [M + H$^+$] calcd for $C_{17}H_{14}FN_5O_5S$: 420.0773. Observed: 420.0769.

dx.doi.org/10.1021/jm4006719 | J. Med. Chem. XXXX, XXX, XXX−XXX

(2*S*,3*S*)-3-((*S*)-1-Oxo-1-(phenylamino)-3-(thiazol-4-yl)-propan-2-ylcarbamoyl)oxirane-2-carboxylic Acid (30). The general saponification procedure was followed using the corresponding peptidomimetic epoxide ethyl ester **16a** (112 mg, 0.28 mmol), LiOH (6.9 mg, 0.29 mmol), and THF/MeOH/H_2O (2.5 mL/1.0 mL/1.0 mL), yielding **30** as a white solid (45 mg, 43.3%). ^{1}H NMR (MeOD-d_4, 400 MHz,): δ 8.97 (s, 1H); 7.52−7.50 (d, 2H); 7.32 (s, 1H); 7.30−7.26 (t, 3H); 4.94−4.92 (t, 1H); 3.62 (s, 1H); 3.52−3.45 (q, 2H); 3.43 (s, 1H). ^{13}C NMR (DMSO-d_6, 100 MHz): δ 172.48, 169.65, 168.87, 153.83, 152.41, 138.16, 128.33, 124.04, 120.73, 115.89, 54.49, 53.60, 52.89 32.87. ESI-HRMS (m/z) [M + H$^+$] calcd for $C_{16}H_{15}N_3O_5S$: 360.0660. Observed: 360.0673. HPLC method 2: t_R = 16.4 min; purity = 95.2%.

3-((*S*)-1-(4-(4-Fluorophenyl)thiazol-2-ylamino)-1-oxo-3-(thiazol-4-yl)propan-2-ylcarbamoyl)oxirane-2-carboxylic Acid (31). The general saponification procedure was followed using the corresponding peptidomimetic epoxide ethyl ester **16b** (974 mg, 2.0 mmol), LiOH (47.5 mg, 2.0 mmol), and THF/MeOH/H_2O (25 mL/5 mL/2 mL), yielding **31** as a white solid (685 mg, 74.6%). ^{1}H NMR (MeOD-d_4, 400 MHz,): δ 8.99−8.98(d, 1H, J = 1.67 Hz); 7.94−7.91 (q, 2H); 7.37 (s, 1H); 7.36 (s, 1H); 7.15−7.10 (t, 2H); 5.06−5.02 (q, 1H); 3.64−3.63 (d, 1H, J = 1.57 Hz); 3.49−3.45 (m, 3H). ^{13}C NMR (MeOD-d_4, 100 MHz): δ 170.05, 169.01, 166.19, 163.43, 158.19, 154.25, 152.66, 148.36, 131.30, 128.18, 116.63, 116.15, 115.93, 108.62, 53.12, 53.05, 52.21, 33.09. ESI-HRMS (m/z) [M + H$^+$] calcd for $C_{19}H_{15}FN_4O_5S_2$: 463.0541. Observed: 463.0545. HPLC method 2: t_R = 13.7 min; purity = 96.3%.

(2*S*,3*S*)-3-((*S*)-1-(4-(4-Ethynylphenyl)thiazol-2-ylamino)-1-oxo-3-(thiazol-4-yl)propan-2-ylcarbamoyl)oxirane-2-carboxylic Acid (32). The general saponification procedure was followed using **16c** (115 mg, 0.23 mmol), LiOH (6.7 mg, 0.28 mmol), and THF/MeOH/H_2O (4.5 mL/1.5 mL/1.5 mL), yielding **32** as a white solid (48 mg, 44.2%). ^{1}H NMR (DMSO-d_6, 400 MHz): δ 12.57 (s, 1H); 9.06−9.05 (d, 1H, J = 1.92 Hz); 8.81−8.79 (d, 1H, J = 7.8 Hz); 7.93−7.91 (d, 2H, J = 8.4 Hz); 7.76 (s, 1H); 7.55−7.53 (d, 2H, J = 8.4 Hz); 7.45−7.44 (d, 1H, 1.8 Hz); 4.98−4.93 (q, 1H); 4.25 (s, 1H); 3.66−3.65 (d, 1H, J = 1.8 Hz); 3.42−3.41 (d, 1H, J = 1.8 Hz); 3.35−3.22 (m, 2H). ^{13}C NMR (DMSO-d_6, 100 MHz): δ 170.08, 169.03, 165.98, 158.25, 154.33, 152.54, 148.47, 134.95, 132.61, 126.26, 121.32, 116.75, 110.20, 83.87, 81.99, 53.15, 53.08, 51.88, 33.05. ESI-HRMS (m/z) [M + H$^+$] calcd for $C_{21}H_{16}N_4O_5S_2$: 469.0635; observed, 469.0627. HPLC method 1: t_R = 12.5 min, purity = 95.7%.

(2*S*,3*S*)-3-((*S*)-1-(4-(4-Fluorophenyl)thiazol-2-ylamino)-3-(1-methyl-1*H*-imidazol-5-yl)-1-oxopropan-2-ylcarbamoyl)-oxirane-2-carboxylic Acid (33). The general saponification procedure was followed using the corresponding peptidomimetic epoxide ethyl ester **17** (129 mg, 0.26 mmol), LiOH (6.3 mg, 0.26 mmol), and THF/MeOH/H_2O (2.5 mL/1.5 mL/1.5 mL), yielding **33** as a white solid (56 mg, 46.1%). ^{1}H NMR (DMSO-d_6, 400 MHz): δ 8.92−8.90 (d, 1H); 7.96−7.91 (m, 2H); 7.68 (s, 1H); 7.35−7.24 (m, 3H); 4.94−4.87 (m, 1H); 4.64−4.56 (m, 2H); 3.82−3.50 (m, 5H). ^{13}C NMR (400 MHz, DMSO-d_6): δ 171.52, 167.50, 165.57, 162.45, 161.02, 148.42, 138.62, 131.27, 128.18, 128.01, 127.83, 127.05, 116.17, 115.99, 106.70, 53.24, 52.58, 51.90, 31.29, 29.52. ESI-HRMS (m/z) [M + H$^+$] calcd for $C_{20}H_{18}FN_5O_5S$: 460.1085; observed, 460.1092. HPLC method 1: t_R = 17.8 min, purity = 93.6%.

(2*S*,3*S*)-3-((*S*)-1-(4-(4-Fluorophenyl)thiazol-2-ylamino)-3-(1-methyl-1*H*-imidazol-4-yl)-1-oxopropan-2-ylcarbamoyl)-oxirane-2-carboxylic Acid (34). The general saponification procedure was followed using the corresponding peptidomimetic epoxide ethyl ester **18** (93 mg, 0.19 mmol), LiOH (4.5 mg, 0.19 mmol), and THF/MeOH/H_2O (1.5 mL/0.5 mL/0.5 mL), yielding **34** as a white solid (29 mg, 33.1%). ^{1}H NMR (400 MHz, DMSO-d_6): δ 12.50 (bs, 1H), 8.82−8.80 (d, 1H); 7.93−7.91 (m, 2H); 7.76 (s, 1H); 7.63 (s, 1H); 7.46−7.24 (t, 2H); 6.99 (s, 1H); 4.79−4.74 (m, 1H); 3.67−3.66 (d, 1H); 3.62 (s, 3H); 3.49−3.48 (d, 1H); 3.12−2.90 (m, 2H). ^{13}C NMR (400 MHz, DMSO-d_6): δ 169.72, 168.60, 165.56, 162.97, 160.54, 157.78, 147.88, 137.17, 130.84, 127.71, 127.63, 118.35, 115.68, 115.47, 108.08, 53.07, 52.98, 51.56, 33.11, 29.60. ESI-HRMS (m/z) [M + H$^+$] calcd for $C_{20}H_{18}FNO_5S$: 460.1085. Observed: 460.1090. HPLC method 1: t_R = 18.1 min, purity = 95.3%.

Preparation of the Alkynyl Epoxide Ester for Click Derivatization, 19. 19 was generated using the optimized peptide coupling procedure using Boc-protected peptidomimetic (740 mg, 3.5 mmol), (2*S*,3*S*)-epoxysuccinic acid monoester (564 mg, 3.52 mmol), DIPEA (1.53 mL, 8.8 mmol), EDCI (740 mg, 3.9 mmol), and HOBT (520 mg, 3.9 mmol) in DMF (10 mL), affording the title compound (960 mg, 77.6%) as a white solid.

(2*S*,3*S*)-Ethyl 3-((*S*)-1-Oxo-1-(prop-2-ynylamino)-3-(thiazol-4-yl)propan-2-ylcarbamoyl)oxirane-2-carboxylate (19). ^{1}H NMR ($CDCl_3$, 400 MHz): δ 8.78 (s, 1H); 7.65−7.63 (d, 1H, J = 1.00 Hz); 7.14 (s, 1H); 7.04 (bs, 1H); 4.80−4.75 (q, 1H); 4.29−4.24 (m, 2H); 3.99−3.97 (q, 2H); 3.72−3.71 (d, 1H, J = 1.6 Hz); 3.53−3.52 (d, 1H, J = 1.6 Hz); 3.34−3.15 (m, 2H); 2.19 (bs, 1H); 1.33−1.30 (t, 3H). ^{13}C NMR ($CDCl_3$, 100 MHz): δ 169.59, 166.49, 166.45, 153.22, 152.42, 116.20, 78.98, 71.59, 62.31, 53.77, 52.81, 52.44, 32.65, 29.20, 14.02.

General Procedure for Huisgen Cycloaddition To Give the Intermediate Esters (35E−44E). The appropriate arylazide (1.2 equiv) and **19** (1.0 equiv) were dissolved in *t*-BuOH/EtOH/H_2O (1:1:0.5). $CuSO_4$ (0.2 equiv), sodium ascorbate (0.4 equiv), and a catalytic amount of TBTA (0.01 equiv) were added sequentially, and the mixture was stirred for 12 h. The resulting precipitate was filtered off, dissolved in CH_2Cl_2, filtered through Celite, and concentrated in vacuo to afford the desired product in yields and quantities as follows.

(2*S*,3*S*)-Ethyl 3-((*S*)-1-Oxo-1-(1-phenyl-1*H*-1,2,3-triazol-4-yl)-methylamino)-3-(thiazol-4-yl)propan-2-ylcarbamoyl)oxirane-2-carboxylate (35E). The general click procedure was used substituting the following quantities **19** (25.0 mg, 0.08 mmol), phenylazide (9.5 mg, 0.07 mmol), $CuSO_4$ (2.0 mg, 0.01 mmol), NaAsc (6.0 mg, 0.03 mmol), and TBTA (5.0 mg, 0.01 mmol) in *t*-BuOH/EtOH/H_2O (2:1:0.5), affording **35E** as a white solid (32 mg, 92.6%). ^{1}H NMR ($CDCl_3$, 400 MHz): δ 8.74−7.73 (d, 1H, J = 1.90 Hz), 7.93 (s, 1H); 7.73−7.71 (d, 3H, J = 8.68 Hz); 7.55−7.52 (t, 2H); 7.47−7.39 (m, 2H); 7.07−7.06 (d, 1H, J = 1.71 Hz); 4.84−4.79 (q, 1H); 4.56−4.54 (d, 2H, J = 5.87 Hz); 4.32−4.21 (m, 2H); 3.71−3.70 (d, 1H, J = 1.78 Hz); 3.57−3.56 (d, 1H, J = 1.78 Hz); 3.39−3.18 (m, 2H); 1.33−1.31 (t, 3H). ^{13}C NMR ($CDCl_3$, 100 MHz): δ 170.06, 166.52, 166.39, 153.25, 152.36, 145.11, 136.91, 129.75, 128.81, 120.57, 120.46, 115.97, 62.27, 53.80, 52.79, 52.58, 34.98, 32.76, 14.01.

(2*S*,3*S*)-Ethyl 3-((*S*)-1-((1-(4-Fluorophenyl)-1*H*-1,2,3-triazol-4-yl)methylamino)-1-oxo-3-(thiazol-4-yl)propan-2-ylcarbamoyl)-oxirane-2-carboxylate (36E). The general click procedure was used substituting the following quantities **19** (27.3 mg, 0.08 mmol), 1-azido-4-fluorobenzene (10.4 mg, 0.08 mmol), $CuSO_4$ (2.0 mg, 0.01 mmol), NaAsc (6.0 mg, 0.03 mmol), and TBTA (5.0 mg, 0.01 mmol) in *t*-BuOH/EtOH/H_2O (2:1:0.5), affording **36E** as a white solid (35 mg, 92.2%). ^{1}H NMR ($CDCl_3$, 400 MHz): δ 8.73−8.72 (d, 1H, J = 1.91 Hz); 7.90 (s, 1H); 7.74−7.67 (m, 3H); 7.58−7.55 (t, 1H); 7.24−7.18 (t, 2H); 7.07−7.06 (d, 1H, J = 1.71 Hz); 4.84−4.79 (q, 1H); 4.54−4.50 (d, 2H, J = 5.90 Hz); 4.29−4.21 (m, 2H); 3.68−3.67 (d, 1H, J = 1.78 Hz); 3.53−3.52 (d, 1H, J = 1.78 Hz); 3.37−3.18 (m, 2H); 1.30−1.26 (t, 3H). ^{13}C NMR ($CDCl_3$, 100 MHz): δ 169.82, 166.17, 166.03, 163.28, 160.81, 152.86, 152.00, 144.94, 132.78, 122.10, 122.01, 120.48, 116.45, 116.22, 115.59, 61.91, 53.43, 52.40, 52.24, 34.55, 32.42, 13.63.

(2*S*,3*S*)-Ethyl 3-((*S*)-1-Oxo-1-((1-(4-(piperidin-1-ylsulfonyl)-phenyl)-1*H*-1,2,3-triazol-4-yl)methylamino)-3-(thiazol-4-yl)-propan-2-ylcarbamoyl)oxirane-2-carboxylate (37E). The general click procedure was used substituting the following quantities **19** (28.1 mg, 0.08 mmol), 4-piperidinophenylazide (10.7 mg, 0.08 mmol), $CuSO_4$ (3.0 mg, 0.02 mmol), NaAsc (6.0 mg, 0.03 mmol), and TBTA (5.0 mg, 0.01 mmol) in *t*-BuOH/EtOH/H_2O (2:1:0.5), affording **37E** as a white solid (31 mg, 79.8%). ^{1}H NMR ($CDCl_3$, 400 MHz): δ 8.76−8.75 (d, 1H, J = 1.84 Hz); 8.05 (s, 1H); 7.93 (s, 4H); 7.76−7.74 (d, 1H, J = 7.04 Hz); 7.38−7.36 (t, 1H); 7.10−7.09 (d, 1H, J = 1.70 Hz); 4.79−4.76 (q, 1H); 4.58−4.55 (q, 2H); 4.30−4.25 (m, 2H); 3.72−3.71 (d, 1H, J = 1.78 Hz); 3.55−3.54 (d, 1H, J = 1.78 Hz); 3.38−3.17 (abq, 2H); 3.07−304 (t, 3H); 1.75−1.60 (m, 1H); 1.31−1.26 (t, 3H). ^{13}C NMR ($CDCl_3$, 100 MHz): δ 170.31, 169.65, 166.52, 166.44, 153.30, 152.40, 152.34, 145.93, 139.64, 136.68, 129.40, 120.61, 120.41, 116.20, 116.02, 79.01, 71.57, 62.31, 53.77, 52.80, 52.45, 46.94, 32.70, 29.19, 25.11, 23.42, 14.02.

dx.doi.org/10.1021/jm4006719 | J. Med. Chem. XXXX, XXX, XXX−XXX

(2*S*,3*S*)-Ethyl 3-((*S*)-1-(1-(Benzo[*d*][1,3]dioxol-5-yl)-1*H*-1,2,3-triazol-4-yl)methylamino)-1-oxo-3-(thiazol-4-yl)propan-2-ylcarbamoyl)oxirane-2-carboxylate (38E). The general click procedure was used substituting the following quantities **19** (25.0 mg, 0.07 mmol), 5-azidobenzo[*d*][1,3]dioxole (9.5 mg, 0.07 mmol), $CuSO_4$ (2.0 mg, 0.01 mmol), NaAsc (6.0 mg, 0.03 mmol), and TBTA (5.0 mg, 0.01 mmol) in *t*-BuOH/EtOH/H_2O (2:1:0.5), affording **38E** as a white solid (31 mg, 89.7%). ^{1}H NMR ($CDCl_3$, 400 MHz): δ 8.76−8.75 (d, 1H, J = 1.86 Hz); 7.79 (s, 1H); 7.73−7.71 (d, 1H, J = 7.16 Hz); 7.24−7.21 (dd, 2H); 7.14−7.11 (dd, 1H); 7.08−7.07 (d, 1H, J = 1.63 Hz); 6.93−6.91 (d, 1H, J = 8.32 Hz); 6.09 (s, 2H); 4.79−4.76 (q, 1H); 4.54−4.53 (d, 2H, J = 5.90 Hz); 4.31−4.25 (m, 2H); 3.72−3.71 (d, 1H, J = 1.76 Hz); 3.55−3.54 (d, 1H, J = 1.76 Hz); 3.38−3.15 (ab, 2H, J = 92.8 Hz, 57.57 Hz); 1.35−1.30 (t, 3H). ^{13}C NMR ($CDCl_3$, 100 MHz): δ 169.49, 169.05, 164.22, 155.01, 153.30, 148.84, 147.92, 148.27, 130.98, 121.72, 116.26, 114.17, 109.12, 102.60, 102.33, 62.14, 52.95, 52.54, 51.90, 34.78, 33.49, 14.23.

(2*S*,3*S*)-Ethyl 3-((*S*)-1-Oxo-1-((1-(4-sulfamoylphenyl)-1*H*-1,2,3-triazol-4-yl)methylamino)-3-(thiazol-4-yl)propan-2-ylcarbamoyl)oxirane-2-carboxylate (39E). The general click procedure was used substituting the following quantities **19** (109.0 mg, 0.31 mmol), 4-azidobenzenesulfonamide (61.5 mg, 0.31 mmol), $CuSO_4$ (10.0 mg, 0.06 mmol), NaAsc (20.0 mg, 0.03 mmol), and TBTA (10.0 mg, 0.02 mmol) in *t*-BuOH/EtOH/H_2O (4:4:2), affording **39E** as a white solid (119 mg, 69.8%). ^{1}H NMR ($CDCl_3$, 400 MHz): δ 8.93 (s, 1H); 8.45 (s, 1H); 8.19−8.05 (q, 4H); 7.33 (s, 1H); 4.81−4.77 (t, 1H); 4.57−4.48 (q, 2H); 4.28−4.23 (q, 2H); 3.64 (s, 1H); 3.50 (s, 1H); 3.40−3.21 (m, 2H); 1.28−1.23 (t, 3H). ^{13}C NMR (MeOD-d_4, 100 MHz): δ 170.94, 166.80, 166.72, 153.45, 151.92, 145.70, 143.49, 138.85, 127.31, 120.74, 119.76, 115.56, 61.42, 52.72, 52.67, 51.47, 33.93, 31.91, 12.52.

(2*S*,3*S*)-Ethyl 3-((*S*)-1-((1-(3,5-Bis(trifluoromethyl)phenyl)-1*H*-1,2,3-triazol-4-yl)methylamino)-1-oxo-3-(thiazol-4-yl)propan-2-ylcarbamoyl)oxirane-2-carboxylate (40E). The general click procedure was used substituting the following quantities **19** (93.7 mg, 0.27 mmol), 1-azido-3,5-bis(trifluoromethyl)benzene (82.5 mg, 0.32 mmol), $CuSO_4$ (0.6 mg, 0.01 mmol), NaAsc (3.5 mg, 0.02 mmol), and TBTA (15.0 mg, 0.03 mmol) in *t*-BuOH/EtOH/H_2O (4:4:2) with an additional 3 drops of DMF, affording **40E** as a white solid (142 mg, 87.8%). ^{1}H NMR ($CDCl_3$, 400 MHz): δ 8.77 (s, 1H); 8.25 (s, 2H); 8.09 (s, 1H); 7.96 (s, 1H); 7.77−7.75 (d, 1H, J = 7.09 Hz); 7.34−7.32 (t, 1H); 7.11 (s, 1H); 4.81−4.76 (q, 1H); 4.59−4.57 (d, 2H, J = 5.90 Hz); 4.31−4.25 (m, 2H); 3.72−3.711 (d, 1H, J = 1.64 Hz); 3.55−3.54 (d, 1H, J = 1.64 Hz); 3.41−3.17 (m, 2H); 1.01−0.99 (t, 3H). ^{13}C NMR (DMSO-d_6, 100 MHz): δ 170.62, 167.49, 165.37, 154.06, 153.24, 146.92, 138.31, 124.57, 122.37, 121.85, 121.09, 116.21, 61.97, 53.44, 52.97, 51.74, 34.64, 33.49, 14.29.

(2*S*,3*S*)-Ethyl 3-((*S*)-1-((1-(4-Bromophenyl)-1*H*-1,2,3-triazol-4-yl)methylamino)-1-oxo-3-(thiazol-4-yl)propan-2-ylcarbamoyl)oxirane-2-carboxylate (41E). The general click procedure was used substituting the following quantities **19** (60 mg, 0.17 mmol), 1-azido-4-bromobenzene (51 mg, 0.26 mmol), $CuSO_4$ (4.4 mg, 0.03 mmol), NaAsc (22 mg, 0.11 mmol), and TBTA (20.0 mg, 0.04 mmol) in *t*-BuOH/EtOH/H_2O (2:2:1), affording **41E** as a white solid (40 mg, 42.6%). ^{1}H NMR (DMSO-d_6, 400 MHz): δ 9.00−8.99 (d, 1H, J = 1.66 Hz); 8.74−8.71 (t, 1H); 8.63−8.61 (d, 1H, J = 8.22 Hz); 8.54 (s, 1H); 7.60−7.56 (d, 2H, J = 14.85 Hz); 7.345−7.341 (d, 1H, J = 1.63 Hz); 7.11−7.07 (d, 2H, J = 14.85 Hz); 4.69−4.66 (q, 1H); 4.40−4.38 (d, 2H, J = 5.59 Hz); 4.20−4.13 (m, 2H); 3.66−3.66 (d, 1H, J = 1.73 Hz); 3.52−3.51 (d,1H, J = 1.73 Hz); 3.33−3.12 (m, 2H); 1.23−1.20 (t, 3H). ^{13}C NMR (100 MHz, DMSO-d_6): δ 170.57, 167.51, 165.36, 154.07, 153.27, 146.56, 139.39, 136.25, 122.30, 121.54, 117.51, 116.23, 61.97, 53.46, 52.99, 51.76, 34.75, 33.50, 14.32.

(2*S*,3*S*)-Ethyl 3-((*S*)-1-((1-(4-Nitrophenyl)-1*H*-1,2,3-triazol-4-yl)methylamino)-1-oxo-3-(thiazol-4-yl)propan-2-ylcarbamoyl)oxirane-2-carboxylate (42E). The general click procedure was used substituting the following quantities **19** (60 mg, 0.17 mmol), 1-azido-4-nitrobenzene (42 mg, 0.26 mmol), $CuSO_4$ (4.4 mg, 0.03 mmol), NaAsc (22 mg, 0.11 mmol), and TBTA (20.0 mg, 0.04 mmol) in *t*-BuOH/EtOH/H_2O (2:2:1), affording **42E** as an orange solid (40 mg, 45.6%). ^{1}H NMR (DMSO-d_6, 400 MHz): δ 9.00−8.99 (d, 1H, J = 1.8 Hz); 8.77−8.74 (t, 1H); 8.73 (s, 1H); 8.63−8.61 (d, 1H, J = 8.17 Hz); 8.47−8.44 (d, 2H, J = 9.13 Hz); 8.21−8.19 (d, 2H, J = 9.13 Hz); 7.36 (d, 1H, J = 1.78 Hz); 4.71−4.65 (q, 1H); 4.42−4.40 (d, 2H, J = 5.50 Hz); 4.20−4.09 (m, 2H); 3.66−3.65 (d, 1H, J = 1.75 Hz); 3.52−3.51 (d, 1H, J = 1.75 Hz); 3.28−3.06 (m, 2H); 1.22−1.17 (t, 3H). ^{13}C NMR ($CDCl_3$, 100 MHz): δ 170.25, 167.14, 165.00, 153.70, 152.87, 146.77, 146.68, 140.89, 125.70, 121.59, 120.42, 115.86, 61.60, 53.09, 52.61, 51.40, 34.32, 33.12, 13.94.

(2*S*,3*S*)-Ethyl 3-((*S*)-1-((1-(2,6-Difluorophenyl)-1*H*-1,2,3-triazol-4-yl)methylamino)-1-oxo-3-(thiazol-4-yl)propan-2-ylcarbamoyl)oxirane-2-carboxylate (43E). The general click procedure was used substituting the following quantities **19** (48 mg, 0.14 mmol), 2-azido-1,3-difluorobenzene (24 mg, 0.15 mmol), $CuSO_4$ (3.5 mg, 0.02 mmol), NaAsc (18 mg, 0.09 mmol), and TBTA (12 mg, 0.01 mmol) in *t*-BuOH/EtOH/H_2O (1:1:0.5), affording **43E** as a white solid (20 mg, 31.6%). ^{1}H NMR (DMSO-d_6, 400 MHz): δ 8.74−8.73 (d, 1H, J = 1.79 Hz); 7.74−7.72 (m, 2H); 7.55−7.45 (m, 1H); 7.34−7.32 (m, 1H); 7.17−7.13 (t, 2H); 7.04−7.03 (d, 1H, J = 1.72 Hz); 4.82−4.80 (q, 1H); 4.57−4.56 (d, 2H, J = 5.97 Hz); 4.29−4.24 (m, 2H); 3.71−3.70 (d, 1H, J = 1.78 Hz); 3.55−3.54 (d, 1H, J = 1.78 Hz); 3.35−3.18 (m, 2H); 1.33−1.30 (t, 3H). ^{13}C NMR ($CDCl_3$, 100 MHz): δ 170.16, 166.65, 166.30, 158.01, 155.46, 153.29, 152.24, 144.36, 131.48, 129.14, 125.10, 116.01, 112.64, 62.24, 53.81, 52.74, 52.62, 34.74, 32.91, 13.99.

(2*S*,3*S*)-Ethyl 3-((*S*)-1-((1-Mesityl-1*H*-1,2,3-triazol-4-yl)-methylamino)-1-oxo-3-(thiazol-4-yl)propan-2-ylcarbamoyl)-oxirane-2-carboxylate (44E). The general click procedure was used substituting the following quantities **19** (48 mg, 0.14 mmol), 2-azido-1,3-difluorobenzene (24 mg, 0.15 mmol), $CuSO_4$ (3.5 mg, 0.02 mmol), NaAsc (18 mg, 0.09 mmol), and TBTA (12 mg, 0.01 mmol) in *t*-BuOH/EtOH/H_2O (1:1:0.5), affording **44E** as a white solid (30 mg, 42.8%). ^{1}H NMR (400 MHz, DMSO-d_6): δ 8.79−8.74 (d, 1H, J =1.79 Hz); 7.68−7.64 (m, 2H); 7.50 (s, 1H); 7.36−7.34 (d, 2H); 7.28−7.26 (d, 2H), 7.15−7.10 (m, 2H), 6.98 (s, 1H); 5.50 (s, 1H); 4.83−4.78 (m, 1H); 4.59−4.58 (d, 1H); 4.29−4.25 (m, 2H); 3.99−3.97 (q, 1H); 3.81 (s, 3H); 3.69−3.68 (m, 3H); 3.55−3.54 (d, 1H); 3.37−3.19 (abq, 2H); 2.35 (s, 3H); 1.93 (s, 3H) 1.33−1.29 (t, 3H). ^{13}C NMR (DMSO-d_6, 100 MHz): δ 169.25, 165.62, 153.65, 152.98, 144.93, 140.11, 134.51, 134.50, 128.12, 124.69, 115.88, 63.51, 52.69, 52.78, 51.98, 48.66, 34.54, 33.10, 20.69, 16.89, 13.52.

(2*S*,3*S*)-3-((*S*)-1-Oxo-1-((1-phenyl-1*H*-1,2,3-triazol-4-yl)-methylamino)-3-(thiazol-4-yl)propan-2-ylcarbamoyl)oxirane-2-carboxylic Acid (35). The general procedure was followed using the corresponding peptidomimetic epoxide ethyl ester **35E** (23 mg, 0.47 mmol) and LiOH (1.2 mg, 0.05 mmol) and after extraction afforded the desired product as a white solid (18 mg, 84.9%). ^{1}H NMR (DMSO-d_6, 400 MHz): δ 9.00−8.99 (d, 1H, J = 1.76 Hz); 8.73−8.70 (t, 1H); 8.58−8.56 (d, 1H, J = 8.24 Hz); 8.50 (s, 1H); 7.87−7.85 (d, 2H, J = 7.76 Hz); 7.61−7.49 (m, 3H); 7.344−7.341 (d, 1H, J = 1.21 Hz); 4.69−4.66 (q, 1H); 4.41−4.39 (d, 2H, J = 5.49 Hz); 3.59−3.59 (d, 1H, J = 1.58 Hz); 3.35−3.10 (m, 3H). ^{13}C NMR (DMSO-d_6, 100 MHz): δ 170.62, 169.06, 165.75, 154.05, 153.31, 146.36, 137.07, 130.38, 129.06, 131.48, 120.41, 116.19, 53.25, 52.96, 51.90, 34.80, 29.42. HRMS-ESI m/z [M + H$^+$] calcd for $C_{18}H_{16}N_6O_5S$: 443.1137. Observed: m/z 443.1135 (M + H$^+$);. HPLC method 2: t_R = 16.7 min; purity = 97.9%.

(2*S*,3*S*)-3-((*S*)-1-((1-(4-Fluorophenyl)-1*H*-1,2,3-triazol-4-yl)-methylamino)-1-oxo-3-(thiazol-4-yl)propan-2-ylcarbamoyl)-oxirane-2-carboxylic Acid (36). The general procedure was followed using the corresponding peptidomimetic epoxide ethyl ester **36E** (25 mg, 0.51 mmol) and LiOH (1.3 mg, 0.06 mmol) and after extraction afforded the desired product as a white solid (18 mg, 76.2%). ^{1}H NMR (DMSO-d_6, 400 MHz): δ 8.98 (s, 1H); 8.72−8.70 (t, 1H); 8.57−8.55 (d, 1H, J = 8.06); 8.48 (s, 1H); 7.93−7.90 (q, 2H); 7.48−7.44 (t, 2H); 7.34 (s, 1H); 4.70−4.65 (q, 1H); 4.40−4.38 (d, 2H; J = 5.52); 3.66 (s, 1H); 3.54−3.06 (m, 3H). ^{13}C NMR (DMSO-d_6, 100 MHz): δ 170.62, 165.75, 163.24, 160.80, 154.06, 153.32, 146.40, 133.62, 122.81, 122.72, 121.76, 117.33, 117.10, 53.24, 53.01, 52.94, 34.77, 33.50. HRMS-ESI m/z [M + H$^+$] calcd for $C_{19}H_{17}FN_6O_5S$: 461.1043. Observed: m/z 461.1049 (M + H$^+$). HPLC method 2: t_R = 17.9 min; purity = 97.2%.

(2*S*,3*S*)-3-((*S*)-1-Oxo-1-((1-(4-(piperidin-1-ylsulfonyl)phenyl)-1*H*-1,2,3-triazol-4-yl)methylamino)-3-(thiazol-4-yl)propan-2-ylcarbamoyl)oxirane-2-carboxylic Acid (37). The general proce-

dx.doi.org/10.1021/jm4006719 | J. Med. Chem. XXXX, XXX, XXX−XXX

dure was followed using the corresponding peptidomimetic epoxide ethyl ester **37E** (26 mg, 0.42 mmol) and LiOH (1.0 mg, 0.04 mmol) and after extraction afforded the desired product as a white solid (12 mg, 48.3%). ^{1}H NMR (acetone-d_6, 400 MHz): δ 8.98 (bs, 1H); 8.48 (s, 1H); 8.16−8.12 (d, 2H, 8.48); 8.02−8.00 (d, 2H, J = 8.48 Hz); 7.37 (bs, 1H); 4.81 (bs, 1H); 4.52 (s, 2H); 3.85−3.79 (m, 4H); 3.61 (s, 1H); 3.55 (s, 1H); 1.82−1.60 (m, 6H). ^{13}C NMR (acetone-d_6, 100 MHz): δ 170.07, 169.01, 165.12, 153.52, 139.36, 136.19, 129.47, 120.84, 120.21, 107.39, 107.25, 66.62, 53.44, 52.80, 52.77, 46.83, 32.52, 30.07, 25.02, 23.13. HRMS-ESI m/z [M + H$^+$] calcd for $C_{24}H_{27}N_7O_7S_2$: 590.6440. Observed: m/z 590.1050 (M + H$^+$). HPLC method 2: t_R = 21.7 min; purity = 96.3%.

(2*S*,3*S*)-3-((*S*)-1-((1-(Benzo[*d*][1,3]dioxol-5-yl)-1*H*-1,2,3-triazol-4-yl)methylamino)-1-oxo-3-(thiazol-4-yl)propan-2-ylcarbamoyl)oxirane-2-carboxylic Acid (38). The general procedure was followed using the corresponding peptidomimetic epoxide ethyl ester **38E** (10 mg, 0.16 mmol) and LiOH (0.35 mg, 0.02 mmol) and after extraction afforded the desired product as a white solid (7 mg, 73.1%). ^{1}H NMR (DMSO-d_6, 400 MHz): δ 9.00−8.99 (d, 1H, J = 1.88 Hz); 8.71−8.68 (t, 1H); 8.57−8.55 (d, 1H, J = 8.28 Hz); 8.38 (s, 1H); 7.46−7.45 (d, 1H, J = 2.15 Hz); 7.33−7.31 (m, 2H); 7.11 (s, 1H); 7.09 (s,1H); 6.15 (s, 2H); 4.67−4.65 (m, 1H); 4.38−4.36 (d, 2H); 3.60−3.58 (d, 1H, J = 1.72 Hz); 3.50−3.17 (m, 3H). ^{13}C NMR (DMSO-d_6, 100 MHz): δ 170.59, 169.06, 165.75, 154.05, 153.31, 148.65, 147.81, 146.07, 131.53, 121.69, 116.19, 114.15, 109.11, 102.58, 102.33, 53.24, 52.94, 51.90, 34.78, 33.49. HRMS-ESI m/z [M + H$^+$] calcd for $C_{20}H_{18}N_6O_7S$: 487.4643. Observed: m/z 487.1050 (M + H$^+$); HPLC method 2: t_R = 18.1 min; purity = 97.7%.

(2*S*,3*S*)-3-((*S*)-1-Oxo-1-((1-(4-sulfamoylphenyl)-1*H*-1,2,3-triazol-4-yl)methylamino)-3-(thiazol-4-yl)propan-2-ylcarbamoyl)-oxirane-2-carboxylic Acid (39). The general procedure was followed using the corresponding peptidomimetic epoxide ethyl ester **39E** (30 mg, 0.55 mmol) and LiOH (1.3 mg, 0.055 mmol). The product goes into the aqueous layer during workup. The aqueous layer was washed with CH_2Cl_2 and lyophilized to give the desired product as a white solid (8 mg, 45.1%). ^{1}H NMR (DMSO-d_6, 400 MHz): δ 9.00−8.99 (d, 1H, J = 1.92 Hz); 8.79−8.76 (t, 1H); 8.70−8.68 (d, 1H, J = 8.0 Hz); 8.66 (s, 1H); 8.12−8.01 (m, 4H); 7.55 (s, 2H); 7.36 (s, 1H); 4.70−4.65 (m, 1H); 4.41−4.40 (d, 2H, J = 5.20 Hz); 3.61 (s, 1H); 3.44−3.10 (m, 3H). ^{13}C NMR (DMSO-d_6, 100 MHz): δ 172.25, 170.66, 169.06, 165.74, 154.10, 152.52, 138.29, 146.80, 144.19, 128.01, 121.75, 120.59, 116.29, 53.25, 52.98, 51.84, 49.01, 33.43. HRMS-ESI m/z [M + H$^+$] calcd for $C_{19}H_{19}N_7O_7S_2$: 522.0865. Observed: m/z 522.0858 (M + H$^+$). HPLC method 2: t_R = 14.8 min; purity = 95.1%.

(2*S*,3*S*)-3-((*S*)-1-((1-(3,5-Bis(trifluoromethyl)phenyl)-1*H*-1,2,3-triazol-4-yl)methylamino)-1-oxo-3-(thiazol-4-yl)propan-2-ylcarbamoyl)oxirane-2-carboxylic Acid (40). The general procedure was followed using the corresponding peptidomimetic epoxide ethyl ester **40E** (94 mg, 0.15 mmol) and LiOH (3.7 mg, 0.15 mmol) and after extraction afforded the desired product as a white solid (72 mg, 80.3%). ^{1}H NMR (DMSO-d_6, 400 MHz): δ 8.99−8.98 (d, 1H, J = 1.92 Hz); 8.92 (s, 1H); 8.79−8.77 (t, 1H); 8.63 (s, 2H); 8.57−8.55 (d, 1H, J = 8.27 Hz); 8.27 (s, 1H); 7.34−7.33 (d, 1H, J = 1.85 Hz); 4.71−4.66 (m, 1H); 4.43−4.42 (d, 2H, J = 5.67 Hz); 3.58−3.57 (d, 1H, J = 1.73 Hz); 3.36−3.35 (d, 1H, J = 1.70 Hz); 3.28−3.10 (m, 2H). ^{13}C NMR (DMSO-d_6, 100 MHz): δ 170.67, 169.07, 165.80, 154.06, 153.29, 146.93, 138.32, 132.48, 132.14, 122.38, 121.11, 116.18, 53.22, 52.90, 51.96, 34.64, 33.51. HRMS-ESI m/z [M + H$^+$] calcd for $C_{21}H_{16}F_6N_6O_5S$: 579.4443. Observed: m/z 579.0890 (M + H$^+$); m/z 577.0775 (M − H$^+$). HPLC method 2: t_R = 24.5 min; purity = 95.3%.

(2*S*,3*S*)-3-((*S*)-1-((1-(4-Bromophenyl)-1*H*-1,2,3-triazol-4-yl)-methylamino)-1-oxo-3-(thiazol-4-yl)propan-2-ylcarbamoyl)-oxirane-2-carboxylic Acid (41). The general procedure was followed using the corresponding peptidomimetic epoxide ethyl ester **41E** (25 mg, 0.04 mmol) and LiOH (1.1 mg, 0.04 mmol) and after extraction afforded the desired product as a white solid (18 mg, 75.9%). ^{1}H NMR (DMSO-d_6, 400 MHz): δ 8.99−8.98 (d, 1H, J = 1.87 Hz); 8.74−8.71 (t, 1H); 8.58−8.56 (d, 1H, J = 8.27 Hz); 8.54 (s, 1H); 7.86−7.79 (q, 4H); 7.34−7.33 (d, 1H, J = 1.75 Hz); 4.70−4.65 (q, 1H); 4.40−4.38 (d, 2H, J = 5.59 Hz); 3.60−3.59 (d, 1H, J = 1.77 Hz); 3.38−3.37 (d, 1H, J = 1.77 Hz); 3.28−3.10 (m, 2H). ^{13}C NMR (DMSO-d_6, 100 MHz): δ 170.62, 169.08, 165.74, 154.06, 153.29, 146.57, 136.25, 133.27, 122.31, 121.67, 121.54, 116.20, 53.25, 52.94, 51.89, 34.76, 33.49. HRMS-ESI m/z [M + H$^+$] calcd for $C_{19}H_{17}BrN_6O_5S$: 521.34. Observed: m/z 523.0229 (M + H$^+$); m/z 519.0123 (M − H$^+$). HPLC method 2: t_R = 21.8 min; purity = 97.2%

(2*S*,3*S*)-3-((*S*)-1-((1-(4-Nitrophenyl)-1*H*-1,2,3-triazol-4-yl)-methylamino)-1-oxo-3-(thiazol-4-yl)propan-2-ylcarbamoyl)-oxirane-2-carboxylic Acid (42). The general procedure was followed using the corresponding peptidomimetic epoxide ethyl ester **42E** (27 mg, 0.05 mmol) and LiOH (1.2 mg, 0.05 mmol) and after extraction afforded the desired product as a white solid (20 mg, 78.3%). ^{1}H NMR (DMSO-d_6, 400 MHz): δ 9.00−8.99 (d, 1H, J = 1.79 Hz); 8.74−8.71 (t, 1H); 8.59 (s, 1H); 8.48−8.47 (d, 1H, J = 8.42 Hz); 8.47−8.45 (d, 2H, J = 9.15 Hz); 8.21−8.19 (d, 2H, J = 9.15 Hz); 7.34−7.33 (d, 1H, J = 1.78 Hz); 4.69−4.66 (q, 1H); 4.42−4.41 (d, 2H, J = 5.60 Hz); 3.60−3.59 (d, 1H, J = 1.79 Hz); 3.50−3.10 (m, 3H). ^{13}C NMR (DMSO-d_6, 100 MHz): δ 170.68, 169.07, 165.75, 154.10, 153.25, 147.11, 147.05, 141.26, 126.08, 121.95, 120.94, 116.23, 53.24, 52.95, 51.85, 34.69, 33.44. HRMS-ESI m/z [M + H$^+$] calcd for $C_{19}H_{17}N_7O_7S$: 488.4543. Observed: m/z 488.0986 (M + H$^+$); m/z 486.0864 (M − H$^+$). HPLC method 2: t_R = 20.4 min; purity = 93.4%.

(2*S*,3*S*)-3-((*S*)-1-((1-(2,6-Difluorophenyl)-1*H*-1,2,3-triazol-4-yl)methylamino)-1-oxo-3-(thiazol-4-yl)propan-2-ylcarbamoyl)-oxirane-2-carboxylic Acid (43). The general procedure was followed using the corresponding peptidomimetic epoxide ethyl ester **43E** (24 mg, 0.05 mmol) and LiOH (1.1 mg, 0.05 mmol) and after extraction afforded the desired product as a white solid (13 mg, 57.3%). ^{1}H NMR (DMSO-d_6, 400 MHz): δ 9.00−8.99 (d, 1H, J = 1.90 Hz); 8.78−8.76 (t, 1H); 8.60−8.58 (d, 1H, J = 8.29 Hz); 8.27 (s, 1H); 7.77−7.69 (m, 1H); 7.49−7.45 (t, 2H); 7.36−7.27 (m, 2H); 4.71−4.65 (m, 1H); 4.44−4.42 (d, 2H, J = 5.63 Hz); 3.598−3.593 (d, 1H, J = 1.78); 3.360−3.355 (d, 1H, J = 1.78); 3.27−3.22 (m, 2H). ^{13}C NMR (DMSO-d_6, 100 MHz): δ 170.69, 169.07, 165.69, 158.07, 158.04, 155.56, 155.53, 154.05, 153.31, 145.67, 136.62, 129.17, 128.48, 126.17, 116.17, 53.23,, 52.93, 51.83, 34.67, 33.51. HRMS-ESI m/z [M + H$^+$] calcd for $C_{19}H_{16}F_2N_6O_5S$: 479.4343. Observed: m/z 479.0960 (M + H$^+$). HPLC method 2: t_R = 17.32 min; purity = 95.9%.

(2*S*,3*S*)-3-((*S*)-1-((1-Mesityl-1*H*-1,2,3-triazol-4-yl)-methylamino)-1-oxo-3-(thiazol-4-yl)propan-2-ylcarbamoyl)-oxirane-2-carboxylic Acid (44). The general procedure was followed using the corresponding peptidomimetic epoxide ethyl ester **44E** (24 mg, 0.05 mmol) and LiOH (1.1 mg, 0.05 mmol) and after extraction afforded the desired product as a white solid (15 mg, 66.1%). ^{1}H NMR (DMSO-d_6, 400 MHz): δ 8.98−8.97 (d, 1H, J = 1.87 Hz); 8.72−8.70 (t, 1H, J = 11.2 Hz); 8.55−8.53 (d, 1H, J = 8.23 Hz); 7.93 (s, 1H); 7.34 (s, 1H); 7.08 (s, 1H); 4.68−4.63 (m, 1H); 4.42−4.40 (d, 2H, J = 5.50 Hz); 3.61−3.50 (m, 4H); 2.32 (s, 3H); 1.86 (s, 6H). ^{13}C NMR (DMSO-d_6, 100 MHz): δ 170.29, 165.60, 153.65, 152.98, 144.93, 139.46, 134.51, 133.50, 128.90, 124.69, 115.78, 52.79, 52.58, 48.66, 34.54, 33.10, 20.69, 16.89. HRMS-ESI m/z [M + H$^+$] calcd for $C_{22}H_{24}N_6O_5S$: 485.5343. Observed: m/z 485.1622 (M + H$^+$); m/z 483.1600 (M − H$^+$). HPLC method 2: t_R = 23.6 min; purity = 97.4%.

Modeling. Coordinates of calpain protein structures were downloaded from the Protein Data Bank (PDB).[56] Visual inspection of the crystal structures 1KXR and 2ARY was performed using Chimera.[57] Conserved water molecules near the binding site were included and allowed to be toggled on and off during docking. Ligands and the binding sites were prepared in MOE.[58] GOLD[59] was used for docking/scoring and employing default parameters and settings.

■ ASSOCIATED CONTENT

Ⓢ Supporting Information

Further details of synthesis, characterization, protein expression; LC−MS; and selectivity assay. This material is available free of charge via the Internet at http://pubs.acs.org.

dx.doi.org/10.1021/jm4006719 | J. Med. Chem. XXXX, XXX, XXX−XXX

AUTHOR INFORMATION

Corresponding Author

*Phone: 312-355-5282. Fax: 312 996 7107. E-mail: thatcher@uic.edu.

Notes

The authors declare no competing financial interest.

ACKNOWLEDGMENTS

The work was supported by NIH Grant U01 AG028713. Molecular modeling was in part conducted using free academic license for the UCSF Chimera package from the Resource for Biocomputing, Visualization, and Informatics at the University of California, San Francisco (supported by NIH Grant P41 RR-01081).

ABBREVIATIONS USED

AD, Alzheimer's disease; ADMET, absorption, distribution, metabolism, excretion, toxicity; Cal1, calpain; $Cal1_{cat}$, calpain 1 recombinant catalytic domain; Cath, cathepsin; CathB, cathepsin B; DET, diethyl tartrate; EIC, extracted ion chromatogram; EDCI, 1-ethyl-3-(3-dimethylaminopropyl)carbodiimide); GSH, glutathione; HOBT, hydroxybenzotriazole; IAA, iodoacetamide; S/N, signal to noise; TIC, total ion chromatogram; TBTA, tris[(1-benzyl-1*H*-1,2,3-triazol-4-yl)methyl]amine

REFERENCES

(1) Goll, D. E.; Thompson, V. F.; Li, H.; Wei, W. E. I.; Cong, J. The calpain system. *Phys. Rev.* **2003**, *83*, 731−801.

(2) Perlmutter, L. S.; Siman, R.; Gall, C.; Seubert, P.; Baudry, M.; Lynch, G. The ultrastructural localization of calcium-activated protease "calpain" in rat brain. *Synapse* **1988**, *2*, 79−88.

(3) Veeranna; Kaji, T.; Boland, B.; Odrljin, T.; Mohan, P.; Basavarajappa, B. S.; Peterhoff, C.; Cataldo, A.; Rudnicki, A.; Amin, N.; Li, B. S.; Pant, H. C.; Hungund, B. L.; Arancio, O.; Nixon, R. A. Calpain mediates calcium-induced activation of the erk1,2 MAPK pathway and cytoskeletal phosphorylation in neurons: relevance to Alzheimer's disease. *Am. J. Pathol.* **2004**, *165*, 795−805.

(4) Shea, T. B. Restriction of microM-calcium-requiring calpain activation to the plasma membrane in human neuroblastoma cells: evidence for regionalized influence of a calpain activator protein. *J. Neurosci. Res.* **1997**, *48*, 543−550.

(5) Di Rosa, G.; Odrijin, T.; Nixon, R. A.; Arancio, O. Calpain inhibitors: a treatment for Alzheimer's disease. *J. Mol. Neurosci.* **2002**, *19*, 135−141.

(6) Huang, Y.; Wang, K. K. W. The calpain family and human disease. *Trends Mol. Med.* **2001**, *7*, 355−362.

(7) Saatman, K.; Creed, J.; Raghupathi, R. Calpain as a therapeutic target in traumatic brain injury. *Neurotherapeutics* **2010**, *7*, 31−42.

(8) Hong, S. C.; Goto, Y.; Lanzino, G.; Soleau, S.; Kassell, N. F.; Lee, K. S. Neuroprotection with a calpain inhibitor in a model of focal cerebral ischemia. *Stroke* **1994**, *25*, 663−669.

(9) Yamashima, T. Ca^{2+}-dependent proteases in ischemic neuronal death: a conserved "calpain−cathepsin cascade" from nematodes to primates. *Cell Calcium* **2004**, *36*, 285−293.

(10) Pike, B. R.; Flint, J.; Dave, J. R.; Lu, X. C. M.; Wang, K. K. K.; Tortella, F. C.; Hayes, R. L. Accumulation of calpain and caspase-3 proteolytic fragments of brain-derived αII-spectrin in cerebral spinal fluid after middle cerebral artery occlusion in rats. *J. Cereb. Blood Flow Metab.* **2004**, *24*, 98−106.

(11) Randriamboavonjy, V.; Fleming, I. All cut up! The consequences of calpain activation on platelet function. *Vasc. Pharmacol.* **2012**, *56*, 210−215.

(12) Randriamboavonjy, V.; Isaak, J.; Elgheznawy, A.; Pistrosch, F.; Fromel, T.; Yin, X.; Badenhoop, K.; Heide, H.; Mayr, M.; Fleming, I. Calpain inhibition stabilizes the platelet proteome and reactivity in diabetes. *Blood* **2012**, *120*, 415−423.

(13) Shields, D. C.; Schaecher, K. E.; Saido, T. C.; Banik, N. L. A putative mechanism of demyelination in multiple sclerosis by a proteolytic enzyme, calpain. *Proc. Natl. Acad. Sci. U.S.A.* **1999**, *96*, 11486−11491.

(14) Dufty, B. M.; Warner, L. R.; Hou, S. T.; Jiang, S. X.; Gomez-Isla, T.; Leenhouts, K. M.; Oxford, J. T.; Feany, M. B.; Masliah, E.; Rohn, T. T. Calpain-cleavage of α-synuclein: connecting proteolytic processing to disease-linked aggregation. *Am. J. Pathol.* **2007**, *170*, 1725−1738.

(15) Vosler, P.; Brennan, C.; Chen, J. Calpain-mediated signaling mechanisms in neuronal injury and neurodegeneration. *Mol. Neurobiol.* **2008**, *38*, 78−100.

(16) Robertson, L. J. G.; Morton, J. D.; Yamaguchi, M.; Bickerstaffe, R.; Shearer, T. R.; Azuma, M. Calpain may contribute to hereditary cataract formation in sheep. *Invest. Ophthalmol. Visual Sci.* **2005**, *46*, 4634−4640.

(17) Robertson, L. J. G.; Nakajima, E.; Morton, J. D.; David, L. L.; Shearer, T. R.; Azuma, M. Calpain-induced proteolysis in lens epithelial cell death during ovine inherited cataract. *Invest. Ophthalmol. Visual Sci.* **2004**, *45*, 2653.

(18) Govindarajan, B.; Laird, J.; Sherman, R.; Salomon, R. G.; Bhattacharya, S. K. Neuroprotection in glaucoma using calpain-1 inhibitors: regional differences in calpain-1 activity in the trabecular meshwork, optic nerve and implications for therapeutics. *CNS Neurol. Disord: Drug Targets* **2008**, *7*, 295−304.

(19) Pietsch, M.; Chua, K. C.; Abell, A. D. Calpains: attractive targets for the development of synthetic inhibitors. *Curr. Top. Med. Chem.* **2010**, *10*, 270−293.

(20) Donkor, I. O. Calpain inhibitors: a survey of compounds reported in the patent and scientific literature. *Expert Opin. Ther. Pat.* **2011**, *21*, 601−636.

(21) Parkes, C.; Kembhavi, A. A.; Barrett, A. J. Calpain inhibition by peptide epoxides. *Biochem. J.* **1985**, *230*, 509−516.

(22) Sugita, H.; Ishiura, S.; Suzuki, K.; Imahori, K. Inhibition of epoxide derivatives on chicken calcium-activated neutral protease (CANP) in vitro and in vivo. *Biochem. J.* **1980**, *87*, 339−341.

(23) K. Hanada, M. T.; Yamagishi, M.; Ohmura, S.; Sawada, J.; Tanaka, I. Isolation and characterization of E-64, a new thiol protease inhibitor. *Agric. Biol. Chem.* **1978**, *42*, 523−528.

(24) Barrett, A. J.; Kembhavi, A. A.; Brown, M. A.; Kirschke, H.; Knight, C. G.; Tamai, M.; Hanada, K. L-*trans*-Epoxysuccinyl-leucylamido(4-guanidino)butane (E-64) and its analogues as inhibitors of cysteine proteinases including cathepsins B, H and L. *Biochem. J.* **1982**, *201*, 189−198.

(25) Trinchese, F.; Fa, M.; Liu, S.; Zhang, H.; Hidalgo, A.; Schmidt, S. D.; Yamaguchi, H.; Yoshii, N.; Mathews, P. M.; Nixon, R. A.; Arancio, O. Inhibition of calpains improves memory and synaptic transmission in a mouse model of Alzheimer disease. *J. Clin. Invest.* **2008**, *118*, 2796−2807.

(26) Greenbaum, D.; Medzihradszky, K. F.; Burlingame, A.; Bogyo, M. Epoxide electrophiles as activity-dependent cysteine protease profiling and discovery tools. *Chem. Biol.* **2000**, *7*, 569−581.

(27) Greenbaum, D. C.; Arnold, W. D.; Lu, F.; Hayrapetian, L.; Baruch, A.; Krumrine, J.; Toba, S.; Chehade, K.; Brömme, D.; Kuntz, I. D.; Bogyo, M. Small molecule affinity fingerprinting: a tool for enzyme family subclassification, target identification, and inhibitor design. *Chem. Biol.* **2002**, *9*, 1085−1094.

(28) Mladenovic, M.; Ansorg, K.; Fink, R. F.; Thiel, W.; Schirmeister, T.; Engels, B. Atomistic insights into the inhibition of cysteine proteases: first QM/MM calculations clarifying the stereoselectivity of epoxide-based inhibitors. *J. Phys. Chem. B* **2008**, *112*, 11798−11808.

(29) Otto, H. H.; Schirmeister, T. Cysteine proteases and their inhibitors. *Chem. Rev.* **1997**, *97*, 133−172.

(30) Cuerrier, D.; Moldoveanu, T.; Campbell, R. L.; Kelly, J.; Yoruk, B.; Verhelst, S. H.; Greenbaum, D.; Bogyo, M.; Davies, P. L. Development of calpain-specific inactivators by screening of positional scanning epoxide libraries. *J. Biol. Chem.* **2007**, *282*, 9600−9611.

(31) Schirmeister, T. New peptidic cysteine protease inhibitors derived from the electrophilic α-amino acid aziridine-2,3-dicarboxylic acid. *J. Med. Chem.* **1999**, *42*, 560−572.

(32) Miyahara, T.; Shimojo, S.; Toyohara, K.; Imai, T.; Miyajima, M.; Honda, H.; Kamegai, M.; Ohzeki, M.; Kokatsu, J. . Phase I study of EST, a new thiol protease inhibitor—the 2nd report safety and pharmacokinetics in continuous administration. *Rinsho Yakuri* **1985**, *16*, 537−546.
(33) Satoyashi, E. Therapeutic trials on progressive muscular dystrophy. *Intern. Med.* **1992**, *31*, 841−846.
(34) *Scrip* **1992**, 1765.
(35) M. Tamai, K. M.; Omura, S.; Koyama, I.; Ozawa, Y.; Hanada, K. In vitro and in vivo inhibition of cysteine proteases by EST, a new analog of E-64. *J. Pharmacobio-Dyn.* **1986**, *9*, 672−677.
(36) Towatari, T.; Nikawa, T.; Murata, M.; Yokoo, C.; Tamai, M.; Hanada, K.; Katunuma, N. Novel epoxysuccinyl peptides. A selective inhibitor of cathepsin B, in vivo. *FEBS Lett.* **1991**, *280*, 311−315.
(37) Hook, G.; Hook, V. Y.; Kindy, M. Cysteine protease inhibitors reduce brain beta-amyloid and beta-secretase activity in vivo and are potential Alzheimer's disease therapeutics. *Biol. Chem.* **2007**, *388*, 979−983.
(38) Tamai, M.; Omura, S.; Kimura, M.; Hanada, K.; Sugita, H. Prolongation of life span of dystrophic hamster by cysteine proteinase inhibitor, loxistatin (EST). *J. Pharmacobio-Dyn.* **1987**, *10*, 678−681.
(39) Bihovsky, R. Reactions of .alpha.,.beta.-epoxy carbonyl compounds with methanethiolate: regioselectivity and rate. *J. Org. Chem.* **1992**, *57*, 1029−1031.
(40) Saito, S.; Komada, K.; Moriwake, T. . Dietyhl (2*S*,2*R*)-2(*N*-*tert*-butoxycarbonyl)amino-3-hydroxysuccinate. *Org. Synth.* **1996**, *73*, 184.
(41) Moldoveanu, T.; Hosfield, C. M.; Lim, D.; Elce, J. S.; Jia, Z.; Davies, P. L. A Ca^{2+} switch aligns the active site of calpain. *Cell* **2002**, *108*, 649−660.
(42) Moldoveanu, T.; Campbell, R. L.; Cuerrier, D.; Davies, P. L. Crystal structures of calpain-E64 and -leupeptin inhibitor complexes reveal mobile loops gating the active site. *J. Mol. Biol.* **2004**, *343*, 1313−1326.
(43) Cuerrier, D.; Moldoveanu, T.; Inoue, J.; Davies, P. L.; Campbell, R. L. Calpain inhibition by alpha-ketoamide and cyclic hemiacetal inhibitors revealed by X-ray crystallography. *Biochemistry* **2006**, *45*, 7446−7452.
(44) Cuerrier, D.; Moldoveanu, T.; Davies, P. L. Determination of peptide substrate specificity for μ-calpain by a peptide library-based approach. *J. Biol. Chem.* **2005**, *280*, 40632−40641.
(45) Suzuki, K.; Hayashi, H.; Hayashi, T.; Iwai, K. Amino acid sequence around the active site cysteine residue of calcium-activated neutral protease (CANP). *FEBS Lett.* **1983**, *152*, 67−70.
(46) Baumann, M.; Baxendale, I. R.; Ley, S. V.; Nikbin, N. An overview of the key routes to the best selling 5-membered ring heterocyclic pharmaceuticals. *Beilstein J. Org. Chem.* **2011**, *7*, 442−495.
(47) Tamayev, R.; Akpan, N.; Arancio, O.; Troy, C. M.; L, D. A. Caspase-9 mediates synaptic plasticity and memory deficits of Danish dementia knock-in mice: caspase-9 inhibition provides therapeutic protection. *Mol. Neurodegener.* **2012**, *7*, 60.
(48) D'Amelio, M.; Cavallucci, V.; Middei, S.; Marchetti, C.; Pacioni, S.; Ferri, A.; Diamantini, A.; De Zio, D.; Carrara, P.; Battistini, L.; Moreno, S.; Bacci, A.; Ammassari-Teule, M.; Marie, H.; Cecconi, F. Caspase-3 triggers early synaptic dysfunction in a mouse model of Alzheimer's disease. *Nat. Neurosci.* **2011**, *14*, 69−76.
(49) Hook, V. Y.; Kindy, M.; Hook, G. Inhibitors of cathepsin B improve memory and reduce beta-amyloid in transgenic Alzheimer disease mice expressing the wild-type, but not the Swedish mutant, beta-secretase site of the amyloid precursor protein. *J. Biol. Chem.* **2008**, *283*, 7745−7753.
(50) Hook, G.; Hook, V.; Kindy, M. The cysteine protease inhibitor, E64d, reduces brain amyloid-beta and improves memory deficits in Alzheimer's disease animal models by inhibiting cathepsin B, but not BACE1, beta-secretase activity. *J. Alzheimer's Dis.* **2011**, *26*, 387−408.
(51) Wang, C.; Sun, B.; Zhou, Y.; Grubb, A.; Gan, L. Cathepsin B degrades amyloid-beta in mice expressing wild-type human amyloid precursor protein. *J. Biol. Chem.* **2012**, *287*, 39834−39841.
(52) Huo, S.; Wang, J.; Cieplak, P.; Kollman, P. A.; Kuntz, I. D. Molecular dynamics and free energy analyses of cathepsin D-inhibitor interactions: insight into structure-based ligand design. *J. Med. Chem.* **2002**, *45*, 1412−1419.
(53) Danielson, M. L.; Desai, P. V.; Mohutsky, M. A.; Wrighton, S. A.; Lill, M. A. Potentially increasing the metabolic stability of drug candidates via computational site of metabolism prediction by CYP2C9: the utility of incorporating protein flexibility via an ensemble of structures. *Eur. J. Med. Chem.* **2011**, *46*, 3953−3963.
(54) Rydberg, P.; Vasanthanathan, P.; Oostenbrink, C.; Olsen, L. Fast prediction of cytochrome P450 mediated drug metabolism. *ChemMedChem* **2009**, *4*, 2070−2079.
(55) Moors, S. L.; Vos, A. M.; Cummings, M. D.; Van Vlijmen, H.; Ceulemans, A. Structure-based site of metabolism prediction for cytochrome P450 2D6. *J. Med. Chem.* **2011**, *54*, 6098−6105.
(56) Kirchmair, J.; Markt, P.; Distinto, S.; Schuster, D.; Spitzer, G. M.; Liedl, K. R.; Langer, T.; Wolber, G. The Protein Data Bank (PDB), its related services and software tools as key components for in silico guided drug discovery. *J. Med. Chem.* **2008**, *51*, 7021−7040.
(57) Pettersen, E. F.; Goddard, T. D.; Huang, C. C.; Couch, G. S.; Greenblatt, D. M.; Meng, E. C.; Ferrin, T. E. UCSF Chimera—a visualization system for exploratory research and analysis. *J. Comput. Chem.* **2004**, *25*, 1605−1612.
(58) Molecular Operating Environment. http://www.chemcomp.com.
(59) Jones, G.; Willett, P.; Glen, R. C. Molecular recognition of receptor-sites using a genetic algorithm with a description of desolvation. *J. Mol. Biol.* **1995**, *245*, 43−53.

dx.doi.org/10.1021/jm4006719 | *J. Med. Chem.* XXXX, XXX, XXX−XXX